Description of the North Sea Wind climate for offshore wind energy applications

Reference number 91-327
File number 112324-22013
Date November 1991
P

Authors
J.W. Cleijne
J.P. Coelingh
A.J.M. van Wijk

ST-Code
C 19.3

Keywords
– wind energy
– wind data
– offshore

Attended for
NOVEM
Contract: 24401-1010
T.a.v. Ir. E. Luken
Postbus 8242
3503 RE Utrecht

Summary

For the year 2000 the Dutch government aims at an installed wind turbine capacity of 1000 MW. By the year 2010 this should have been increased to 2000 MW, of which 200 MW are to be installed in the North Sea. To be able to erect offshore wind turbines it is necessary to have a description of the offshore wind climate, both for wind energy production estimates as for wind turbine design.

To this end a first initial study of the offshore wind climate has been made, using wind data from the gas production platforms K13 (with wind data over the period 1982-1989) and West Sole (June 1983-May 1984), which are positioned in the southern North Sea.

The aim of the study was to

1. give first estimates of the wind resource and turbulence intensities over the Southern North sea making use of the wind speed data measured at K13 and West Sole,
2. assess the accuracy of the data,
3. if possible, suggest changes to the present methods for the determination of the wind resources near the coast and the design wind load data offshore,
4. make an assessment of the research required to improve the knowledge of the offshore wind resources and design wind load data.

For the mean wind speed measured at K13 at a height of 74.9 meters above Mean Sea Level (MSL), a value of 9.0 m/s has been found. The Weibull shape factor was 2.04. The wind climate at K13 has been compared with the wind climate at Light Vessel Texel in the period 1966-1976. The calculated annual mean wind speed at K13 for a height of 10 m compares quite well with the value at LV Texel. This has lead to the conclusion that, based on the results of K13, the use of LV Texel in the Dutch Handbook for Wind Energy Production Estimates for climatological purposes seems justified.

At K13 the interannual variations of the yearly mean wind speed are between +14% and -16%, which seems to be larger than on land. A pronounced seasonal course in the wind speed was observed. The monthly mean wind speeds deviate from the annual mean wind speed between +26% and -22%. An average maximum of 11.8 m/s occurs in January and a minimum of 7.0 m/s is found in June. No significant diurnal course has been found at K13. The distribution of wind directions of K13 shows that the prevailing wind direction is southwesterly (sector 7 to 10). In these sectors also the maximum wind speeds are found (9.1-10.1 m/s).

Analysis has shown that at K13 unstable conditions for the planetary boundary layer prevail. During the winter the air temperature is lower than the seawater temperature, while in the summer the situation is the other way around. On the average the air temperature was 0.89 °C lower than the seawater temperature.

Transformation of the wind speed from 74.9 m down to 10 m using a diabatic wind profile and a logarithmic wind profile resulted in the same value (±1%), meaning that both models describe the wind profile equally well.

The overall mean calculated roughness length was 0.00017 m, which matches the generally accepted mean value of 0.0002 m. The extreme values, however, ranged from 0.00002 m to 0.00055 m, depending strongly on the wind speed.
The diabatic model for the calculation of wind profiles has been compared with the wind speeds in the West Sole database. The uncertainties in the West Sole temperature database, however, have prevented solid conclusions on the validity of the diabatic model.

The value of the mean geostrophic wind speed at K13, calculated using four different methods, ranged from 10.2 m/s to 10.4 m/s. For Light Vessel Texel nearly the same values have been found. Moreover, these values are in the same range as results given by the European and Danish Wind Atlas. Compared with these results, the results given by Wieringa and Rijkoort [1983] based on land based stations seem too high (13 m/s).
The Planetary Boundary Layer height (PBL) depends on stability conditions. For neutral conditions a mean PBL height of 1123 m has been found, while for very stable conditions the mean PBL height was only 107 m. In very stable conditions the PBL was sometimes lower than the measuring height 74.9 m.

The measurements at West Sole have shown that the turbulence intensity offshore is considerably lower than over land. Above a wind speed of approximately 10 m/s mechanical turbulence dominates over convective turbulence. In that range the turbulence intensity is described well by a simple expression when using the correct roughness length according to the Charnock relation. Typically, a turbulence intensity of 8-10% has been found at all heights. For lower wind speeds the average turbulence intensity is higher, which can be explained by the influence of stability.

A literature survey showed that information on the spectral characteristics of offshore wind is scarce. The experiments described indicate that the power spectra of the turbulent wind follow the well-known Kaimal-spectrum for the higher frequencies, but that at lower frequencies the spectral content is higher in unstable atmospheres and lower in stable atmospheres.
Reports on the fast-rated West Sole experiments seem to indicate that the coherence functions measured there are consistent with those measured on-land.

To estimate the energy production of offshore wind turbines it is necessary to have a description of the wind climate at hub height for the location where a particular wind turbine will be installed.
For the calculation of the wind climate it is necessary

1. to compose a map which describes the geostrophic offshore wind climate.
2. to translate the geostrophic wind climate at the desired location to the wind climate at hub height.

Various methods exist, which can be used to compose a map of the geostrophic wind climate. These methods differ in complexity and therefore it is necessary to assess first the climatological data that is needed.

Maps for the overall mean geostrophic wind speed above the North Sea do exist using pressure field data as an input. Since these maps can only supply average wind speeds, these maps cannot be used to give a more detailed description of the wind climate.
For a more detailed description of the wind climate it is necessary to have

information about the wind speed frequency distribution, the distribution by wind direction, etc. Therefore, it will be necessary to describe these aspects for the geostrophic wind climate as well. These data can only be generated using surface wind speed data.

Although for K13 and LV Texel the same mean geostrophic wind speed has been found, the results show that the Weibull shape factor for the geostrophic wind speed for K13 is not the same as for LV Texel. It is not clear what brings about this difference. Further research using other databases must be carried out to identify the Weibull shape factor for the geostrophic wind speed and its geographical variation. Also other aspects of the geostrophic wind climate require that wind speed databases of other stations be investigated.

For an adequate description of the wind climate it is necessary that the wind climate at heights between 10 m and 120 m can be described. There are indications that for wind energy applications the wind profile relation can be simplified by taking roughness length z_0 as a constant and assuming a logarithmic wind speed profile (neutral). These conclusions are based on a very limited database. Therefore, it is necessary validate the wind profile functions. This can be done be setting up a measuring campaign in which the wind speed will be measured at several heights at one station. One of the existing stations in the Measuring Network North-Sea can probably be used for this purpose.

Description of the coastal transition region is very important, because it will probably be one of the first areas where offshore wind turbines will be erected. Research in this area will also give information on the wind climate in the IJsselmeer.
A description of the wind climate in the transition region also enables the description of the wind climate above land and above sea with one single methodology. This decreases the probability of anomalies, such as discontinuities in the wind energy production estimates near the shore. Since no measuring data exist, it is necessary to place a measuring station in this offshore transition layer. The station must be used to carry out measuring campaigns in order to generate databases for studying the wind profile, the internal boundary layer, roughness length in shallow water, etc.

Wind data for offshore wind turbine design are different from on-shore wind data in a number of aspects. Provisional data are available from the analysis of the K13 database, giving data for the wind speed frequency distribution, the turbulence intensity, the average roughness length and the wind shear. However, these data are affected considerably by the stability of the planetary boundary layer. These effects should be investigated in the future using a reliable set of temperature data.

The expressions for the calculation of the fatigue gust amplitudes, which were derived from the wind speed measurements at Cabauw, are probably not valid under offshore conditions. Offshore measurements are necessary to verify the validity of the expressions or to derive new valid expressions. These measurements could be obtained during a relatively brief measuring campaign. In view of the scarcity of experimental spectra and coherence functions offshore and the uncertainties in the spectra at low frequencies measurements of these functions are necessary in order to supply the data required by a stochastic wind simulator, such as SWIFT.

Since wind speeds are generally higher offshore and turbulence intensities lower it is not exactly known what the final effect is on the extreme wind speeds. A detailed analysis of maximum wind speeds should be combined with estimates of the turbulence intensity at high wind speed in order to obtain the required empirical factors in the handbook. Finally, in the future attention should be paid to design data on sea waves and the interaction of sea waves and wind, especially under storm conditions.

Table of contents

List of symbols

α	gz_0/u_*^2	0.0144
Δz	height difference	m
ε	turbulent dissipation	
κ	Von Kármán constant	0.4
μ	stability parameter (= $u_*/f_{Cor}L$)	-
Φ	geopotential (= gz)	
Ψ	stability function	-
a	Weibull scale factor	m/s
A_g	amplitude of wind shear	
a_z	decay constant	
c_p	phase speed of the dominant wave	m/s
d	grid length	150 km
D	rotor diameter	m
f	frequency	Hz
f(U)	probability density that the wind speed exceeds U	s^{-1}
f_{Cor}	Coriolis parameter	$1.22x10^{-4}$ s^{-1}
f_m	normalized frequency	
g	gravitational constant	9.81 m/s^2
GMT	Greenwich Mean Time	
h	planetary boundary layer height	m
H	hub height	m
I_3	turbulence intensity	-
I_{60}		
k	Weibull shape factor	-
k	turbulent wave number	m^{-1}
k	unit vector in z-direction	
L	Obukhov length	m
LAT	Lowest Astronomical Tide	
MSL	Mean Sea Level	
n	non-dimensional frequency (fz/U)	-
n_i	non-dimensional frequency	-
n_m	normalized frequency (f_m/U)	-
p	air pressure at sea level	hPa
PBL	planetary boundary layer	
T_{air}	air temperature corrected to a height of 2 m above MSL	°C
T_{sea}	seawater temperature measured at the surface	°C
U	wind speed	m/s
u_*	friction velocity	m/s
U_{10}	wind speed at 10 m height	m/s
U_{geo}	geostrophic wind speed	m/s
U_{mean}	mean wind speed	m/s
<U>	median wind speed	m/s
z	height	m
z_0	roughness length	m
z_i	height of lowest inversion	m

1 General introduction

For the year 2000 the Dutch government aims at an installed wind turbine capacity of 1000 MW. By the year 2010 this should have been increased to 2000 MW, of which 200 MW are to be installed offshore in the North Sea.

The main reason for erecting wind turbines offshore is the urge for space, despite the higher cost. The higher cost is partly recovered by the assumed better wind potential over sea.

It is important to know the offshore wind climate for the following reasons:
- Investors must know the wind speed frequency distribution in order to estimate the feasibility of offshore wind energy projects;
- Wind turbine designers require sufficiently accurate design wind load data in order to design safe, reliable and economical machines.

The aim of the present study is to
1. give first estimates of the wind resource and turbulence intensities over the Southern North sea making use of the wind speed data measured at K13 and West Sole,
2. assess the accuracy of the data,
3. suggest changes to the present methods, if possible, for the determination of the wind resources near the coast and the design wind load data offshore,
4. make an assessment of the research required to improve the knowledge of the offshore wind resources and design wind load data.

Several studies have been reported on the North Sea wind climate [e.g. Korevaar, 1989; Moore, 1982; Børresen, 1987; Barthelmie et al., 1990].

There are five different sources of data for offshore wind climate studies. These are:
- Voluntary Observing Ships
- Light Vessels
- Upper air measurements
- Measuring Network North Sea
- Special offshore measuring campaigns

Since long, Voluntary Observing Ships have recorded meteorological measurements. For wind climate studies these measurements are not accurate enough, since
- the frequency of observations is low (at maximum 4 times a day),
- wind speeds are estimated according to Beaufort classification,
- the availability of these data is not sufficient for all areas of the North Sea
- and there is not an adequate check of the quality of these data.

Although for wind climatology these data are of limited value, for some other aspects data of Voluntary Observing Ships can be used. For instance, it is possible to analyze the seawater temperatures using this source (see section 3.4).

Light vessels have also been recording meteorological data for a long time. For wind climatology studies this is probably the most interesting source, although the measurements were carried out using a Beaufort classification. For the Dutch North Sea area wind speeds have been recorded until the 80s.

Upper air measurements are carried out with balloons from several stations several times a day. In principle, long time series of measurements are available. For the Netherlands, however, these measurements are available. For the Netherlands, however, these measurements have not been analysed recently. In the United Kingdom these data have been used to analyze the upper air wind speed field. Only the mean wind speed can be calculated by analysing these data. Nevertheless, it is possible to use the data for the validation of models for the geostrophic wind.

In the late 70s and early 80s in the Netherlands automatic wind speed recording equipment on various offshore locations have been installed, incorporated into the Measuring Network North Sea. This network contains eight coastal and offshore measuring stations, of which K13 is one. Unfortunately, there is no overlapping period of measurements of Light Vessels and from the Network, which means that no accurate comparisons of these sources of data can be made.

In the United Kingdom an offshore measuring campaign has been started in 1978, at the West Sole gas platform. Over a period of more than 10 year data have been collected for scientific purposes from a measuring mast, with anemometers at seven heights.

For this study the K13 and West Sole gas platform have been selected. The K13 platform lies west of the Wadden Islands near the Dutch sea coast, while West Sole is situated more northerly near the British coast.
The K13 platform was selected, because wind speed recordings were made over a relatively long period and because the disturbances of the wind speed due to the tower have been studied in a wind tunnel. The West Sole platform was selected mainly because the wind speed has been measured at seven heights and also turbulence intensities have been recorded. Unfortunately, only recordings over a one year period are available, which means that the data cannot be used for climatological purposes.

Annex 1 gives a summary of coastal stations, light vessels and offshore platforms and some characteristics of the available databases. Figure 1.1 depicts the locations of the stations.

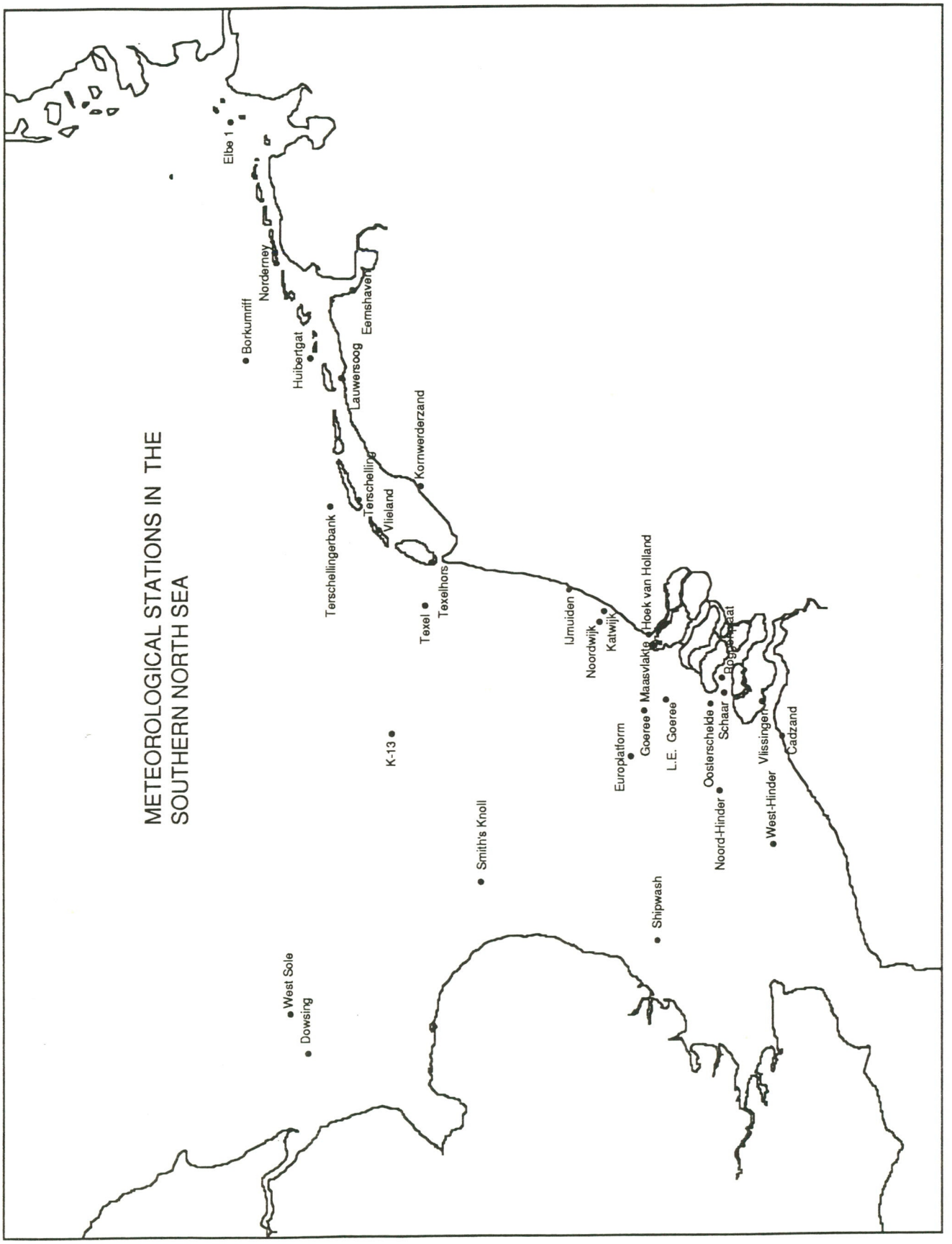

Figure 1.1 Overview of North Sea locations where wind speeds have been recorded

Because the number of stations at which the wind speed is recorded is very limited, it is necessary to develop models, able to transform measured data from one location to another. Chapter 2 discusses
- the diabatic wind profile model used to describe the surface wind, [Van Wijk, 1990],
- four models used to derive the geostrophic wind,
- a model to describe the turbulence intensity.

In the next chapters, these models are applied to the selected databases.

The K13 platform and database are described in chapter 3. The chapter contains the statistical analysis of the measured data, such as frequency distribution, wind direction distribution, stability and Weibull parameters and a comparison among the results of the 4 methods to calculate the geostrophic wind.

Chapter 4 contains the description of the West Sole platform, the collected database and the statistical analysis. Besides the analyses mentioned for the K13 data, the chapter includes an analysis of the wind profile and the turbulence intensity at West Sole.

In the Dutch Handbook for Wind Energy Production Estimates [Verheij et al., 1990] a special procedure is used to estimate the wind speed near the coast. The procedure uses wind data, which were collected at Light Vessel Texel. However, this wind dataset has been based on Beaufort estimates. In chapter 5 the results of the K13 analysis are compared with the Lightship Texel dataset, in order to estimate the accuracy of the latter.

Chapter 6 discusses the subject Wind Data for Wind Turbine Design. It contains a literature review on the spectral characteristics of offshore turbulence. It is expected that this aspect will become more important in the future, in view of the fact that Stochastic Wind Simulators, such as SWIFT, require spectral data as input. Further, the chapter gives an overview of those topics contained in the Handbook Wind Data for Wind Turbine Design, version 3 [Verheij et al., 1991], that would require modification for offshore calculations.

In chapter 7 the conclusions are summarized, an overview is given of topics which need further investigation and recommendations are made for future research.

Acknowledgements

The authors would like to thank the following persons and institutions: J. Wills of British Marine Technology for making available the West Sole database, F.B. Koek and A.W. Donker of Royal Netherlands Meteorological Institute for supplying the databases of K13 and the Voluntary Observing Ships, B. Barthelmie and J. Palutikof of the Climatic Research Unit (University of East Anglia, Norwich), R. Pleune and A. Both for their valuable support.

2 Theory

2.1 Introduction

For wind energy applications the description of the wind up to about 100 m from the earth's surface is important. This falls into the range which is called the planetary boundary layer (PBL). In meteorology, the PBL is usually defined as the layer which is influenced by the surface underneath. Its height varies between about 100 and 1000 m, depending on various conditions. Characteristic for the PBL is the occurrence of turbulent flow.

The PBL consists of two sub-layers: the surface layer (the lowest part, up to about 60 m) and the Ekman layer (the upper part). The most interesting is the surface layer, where the influence of the earth's surface is greatest. By definition, the wind in the layer above the PBL (the troposphere), doesn't depend on the earth's surface anymore but only on pressure differences, and is called the geostrophic wind (or sometimes 'free' wind).

Describing the wind profile, i.e. the wind speed as a function of the height above the earth's surface, is important for wind energy applications. Generally speaking, the wind speed decreases towards the surface (where the wind speed is zero). The reason for this is the influence of the roughness of the surface: the wind flow decreases due to friction. Friction also has an influence on wind direction, the wind direction turns with height.

2.2 Surface wind

The determination of the wind profile is an important subject for wind energy applications. Usually on land the wind speeds are measured at a height of 10 m, but hub heights of wind turbines are expected to be between 30 and 80 m.

A simple and common method of determining the wind profile is by application of the logarithmic wind profile:

$$U(z) = \frac{u^*}{\kappa} ln(\frac{z}{z_0}) \qquad (2.1)$$

with:	u_*	friction velocity
	z_0	roughness length
	κ	Von Kármán constant (0.4)

The roughness length is a parameter which describes the upwind terrain. The wind flow is generally slowed down by obstacles and the roughness of the terrain, which is taken into account by the value of z_0. Above land this value is specific for the type of terrain and does not depend on wind speed. However, in the case of the roughness length experienced by the wind flow at a sea location, the value of z_0 depends on the characteristics of the waves, and therefore on the wind speed.

On this basis Charnock has formulated an expression for z_0 which is used here:

$$z_0 = \alpha \frac{u_*^2}{g} \tag{2.2}$$

with: g gravitational constant
α a constant with a value of 0.0144 [Garratt, 1977].

It must be pointed out that the Charnock relation is only valid when the sea surface is in equilibrium with the wind. This can be understood since the relation doesn't include wave parameters. In case of young waves, i.e. waves developed over a short fetch or stemming from a young wind field, α is no longer constant but depends on the wave age c_p/u_*, in which c_p denotes the phase speed of the dominant wave. In this study it is assumed that the Charnock relation is valid [Maat et al., 1991].

The logarithmic wind profile does not take into account any stability effects, and is in reality only valid in neutral conditions (conditions in which thermal turbulence is negligible compared to mechanical turbulence and there is no vertical heat exchange). To take stability effects into account, the logarithmic wind profile is modified by the addition of the stability function Ψ, resulting in the diabatic wind profile:

$$U(z) = \frac{u_*}{\kappa} \left(ln \left(\frac{z}{z_0} \right) - \Psi \left(\frac{z}{L} \right) \right) \tag{2.3}$$

The stability function Ψ is a function of z and L, where L is the Obukhov length. The parameter L is a measure for the stability. According to Van Wijk [1990], the conditions are defined as neutral if the absolute value of L is greater than 1000 m. For negative values of L (<-1000 m), the conditions are defined as unstable, and for positive values of L (<1000 m), the conditions are defined as stable. To derive the value of L the Monin-Obukhov similarity theory is used. Several formulations have been used for the calculation of Ψ and L. Most of these are valid for situations above land. For situations above sea, Van Wijk [1990] has described a method which leads to a solvable set of equations by using some parametrizations, in such a way that as input only routinely measured data are needed: the wind speed at any height, the air temperature at any height, and the seawater (surface) temperature. By using an iterative procedure, first the values of L, z_0 and u_* can be calculated, and with these the diabatic wind profile is known.

2.3 Geostrophic wind

Theoretically, the validity of Monin-Obukhov similarity theory is limited to the surface layer. However, Van Wijk [1990] has shown it can be used throughout the PBL. By definition, within the PBL the wind profile is influenced by the surface underneath. For that reason the wind above the PBL is called the 'free' wind, or the geostrophic wind. This wind is dependent on pressure differences only.

With the data and the results derived as described before, it is possible to study the geostrophic wind. The geostrophic wind is a 'model' wind, which is calculated from (surface) measurements, or from upper air data. There are several formulations to calculate geostrophic wind speeds, of which four will be used here.

2.3.1 Scaling method

The first one is based on the following notion: physically it can be expected that the wind speed at the top of the PBL is equal to the wind speed just above the PBL, which is the geostrophic wind speed. Although, strictly speaking, Monin-Obukhov similarity theory is only valid in the lower part of the PBL, it has been shown that the results also hold for the upper part of the PBL [Van Wijk, 1990]. Based on this, one of the methods is simply to extrapolate the wind profile to the top of the PBL. This can be expressed by:

$$U_{geo} = U(h) \tag{2.4}$$

where U(h) is the wind speed at the PBL height, calculated with the Monin-Obukhov similarity theory. Therefore the height h of the PBL has to be known, which is (directly or indirectly) a function of L.

In Van Wijk [1990] formulations are given for the value of h. For neutral and stable conditions:

$$h = 0.3\frac{u_*}{f_{Cor}} \qquad \text{for } L \leq 0 \text{ and } |L| \geq 1000 \tag{2.5}$$

with: f_{Cor} Coriolis parameter (1.22×10^{-4} s^{-1}),

and for unstable conditions:

$$h = \frac{L}{3.8}\left\{\sqrt{1 + 2.28\frac{u_*}{f_{Cor}L}} - 1\right\} \qquad \text{for } 0 < L < 1000 \tag{2.6}$$

2.3.2 Geostrophic drag law

The next expression for the geostrophic wind speed is known as the geostrophic drag law [Wieringa and Rijkoort, 1983]. It gives the geostrophic wind speed in neutral conditions, for which case A and B are constants:

$$U_{geo} = \frac{u_*}{\kappa}\sqrt{\left(A - ln\left(\frac{u_*}{z_0 f_{Cor}}\right)\right)^2 + B^2} \tag{2.7}$$

with: A = 1.9, and
B = 4.5

In Lundtang Petersen et al. [1990], a revised form of the geostrophic drag law is presented, where A and B are now functions of the parameter μ, in order to take stability conditions into account:

$$U_{geo} = \frac{u_*}{\kappa}\sqrt{A(\mu) - ln\left(\frac{u_*}{z_0 f_{Cor}}\right)^2 + B^2(\mu)} \qquad (2.8)$$

with: $\mu = \frac{u_*}{f_{Cor}L}$

In the case of neutral conditions when $|L| \rightarrow \infty$, i.e. $\mu \rightarrow 0$, this formulation is identical to the previous one.

2.3.3 Pressure field calculations

The last expression is somewhat different from the previous three. Here, pressure fields have been analysed by Børresen [1987].

The general expression for the (vectorial) geostrophic wind speed is:

$$U_{geo} = \frac{1}{f_{Cor}} k \times \nabla \Phi \qquad (2.9)$$

with: **k** unit vector in z-direction
Φ geopotential (= gz)

A grid with units of 150 km x 150 km has been used, where in each unit pressures at sea level have been used to calculate the 1000 mb heights, according to:

$$z_{1000mb} = 8(p - 1000)\, m \qquad (2.10)$$

with: p air pressure at sea level

The two components of the geostrophic wind can be written as:

$$U_{geo} = \frac{-g}{f_{Cor}2d}(z_{(0,1)} - z_{(0,-1)})$$

$$V_{geo} = \frac{-g}{f_{Cor}2d}(z_{(1,0)} - z_{(-0,-1)}) \qquad (2.11)$$

with: d grid length (150 km)

Here the $z_{(i,j)}$ denote the neighbouring gridpoints of the gridpoint under consideration ($z_{(0,0)}$). Using 27 years of pressure data resulted in a map of the mean geostrophic wind speed of the North Sea, see figure 2.1.

Also shown in the figure are the wind speed values obtained from radiosonde measurements for comparison. These were used to validate the results of the procedure described before. As can be seen, the results over the North Sea match quite well. Over land in Norway, this is not the case, but this can be explained by the presence of mountainous area with heights over 1500 m.

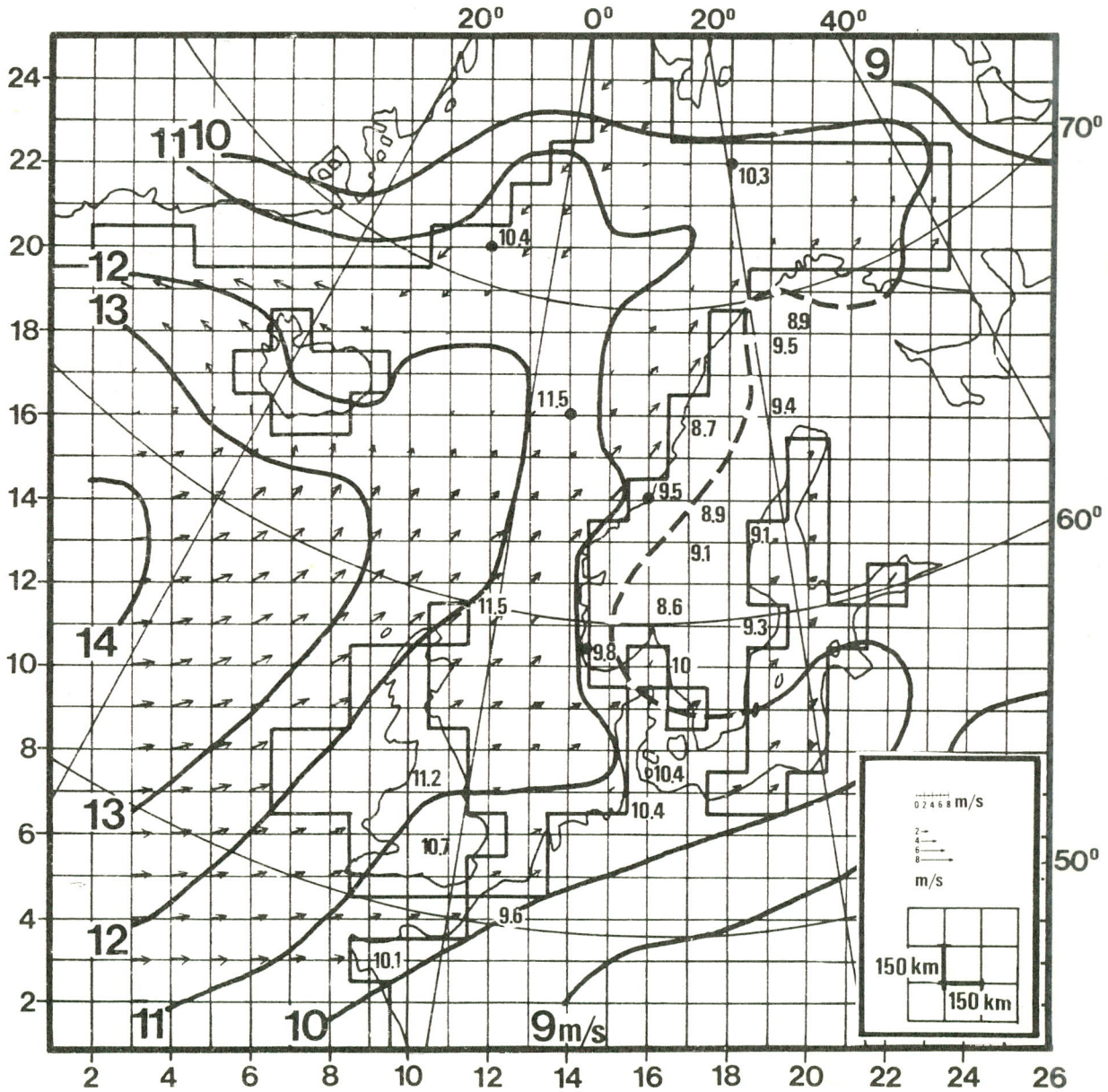

Figure 2.1 Calculated wind field at 1000 m using 27 years of data. Four wind values are available per day. Inserted figures are averages of radiosonde measurements at the 850 mb level [Børresen, 1987]

2.4 Turbulence intensity

Unlike the turbulence intensity over land, the offshore turbulence intensity depends on the wind speed. The reason for this dependence lies in the relation between the friction velocity u_* and the roughness length z_0. The wind speed and the friction velocity are closely related, which will be shown below.

Over land the aerodynamic roughness is closely associated with the physical size of the surface disturbances. Over the sea the aerodynamic roughness is not directly related to the wave height, although this might be thought to be a logical extension of the land case, but rather relates to small wavelets or ripples upon the surface of those waves. The wavelets or ripples depend on wind speed and, therefore, the roughness at sea is itself a function of wind speed.

Under neutral conditions, by definition u_* is constant in the constant stress layer of the PBL.

According to Beljaars [1987] the turbulence intensity I(z) is given by

$$I(z) = \frac{\sigma_U}{U} = \frac{2.2\kappa}{ln(z/z_0)} \qquad (2.12)$$

Over sea, however, z_0 is not a constant according to the Charnock relation (2.2).

Give the wind speed at a certain height and the relations (2.1) and (2.2) we have two equations with two unknowns which can be solved. In this way we find u_* and z_0 both as a function of the wind speed U(z). Figure 2.2 shows u_* and z_0 as functions of the wind speed at 73 m (corresponding to measuring level 2 at West Sole)

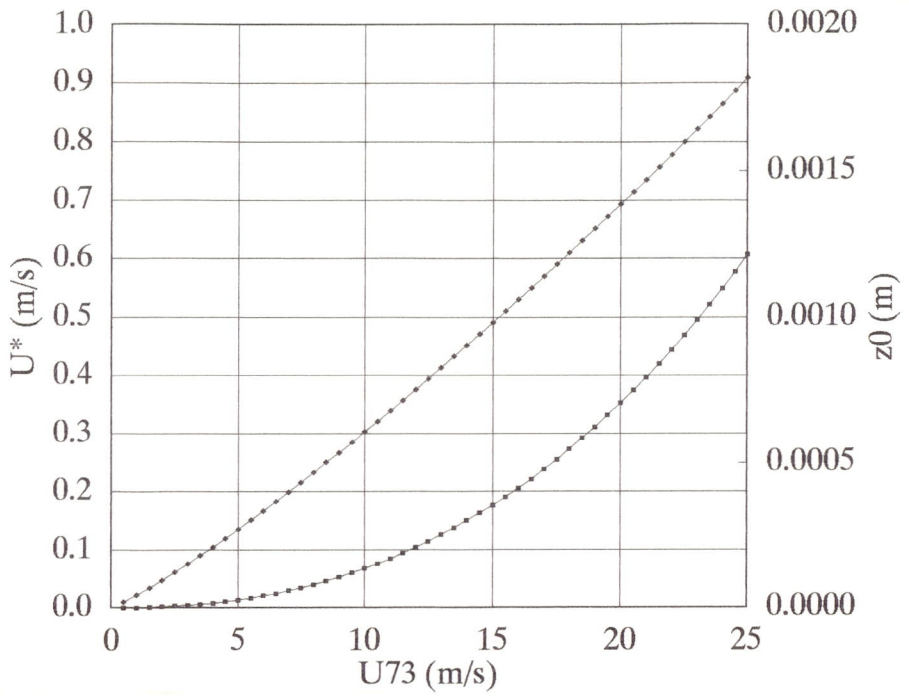

Figure 2.2 Values of U_* (◆) and Z_0 (■) as function of the wind speed at 73 m.

Substitution of $z_0(U)$ of in equation (2.12) yields the turbulence intensity as a function of the wind speed and height. In chapter 4 this is compared with the measured turbulence intensity at West Sole.

In non-neutral situations the turbulence intensity is not well described by the equations given above [Panofsky and Dutton, 1983].

In an unstable atmosphere where convection is added to mechanical turbulence, low frequency variations of large amplitude are observed. It shows that variations in the horizontal plane are independent of height, so that Monin-Obukhov similarity theory cannot be used to describe this phenomenon. Instead, the turbulent fluctuations σ_U depend on the height of the inversion layer z_i, which in our case is taken equal to the height of the PBL h. The wind speed profile U(z) is modified according to (2.3). Hence, Panofsky and Dutton suggest the following expression for the u-component of the turbulence intensity.
In a stable atmosphere the thermal stratification of the atmosphere suppresses turbulence.

$$\frac{\sigma_U}{U} = \frac{\kappa\,(12 - 0.5\,(z_i/L))^{1/3}}{ln\,(z/z_0) - \Psi\,(z/L)} \qquad (2.13)$$

Hence the turbulence intensity is lower. For situations where z/L is not too large, the turbulence intensity is given by

$$\frac{\sigma_U}{U} = \frac{2.2\kappa}{ln(z/z_0) - \Psi(z/L)} \qquad (2.14)$$

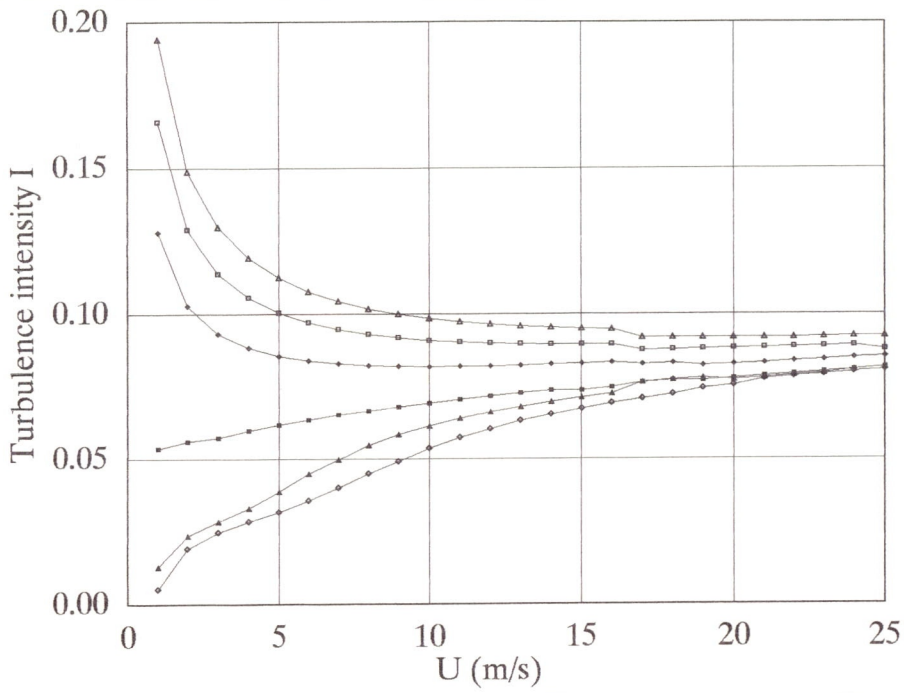

Figure 2.3 The influence of stability on turbulence intensity. Using a constant seawater temperature of 10°C, the temperature difference has been varied: Δ -3°C, ❐ -2°C, ◆ -1°C, ■ 0°C, ▲ 1°C and ♦ 2°C.

Following the approach of Van Wijk [1990] the parameters in (2.13) and (2.14) can be obtained from the seawater and air temperatures and the wind speed at a given height. Figure 2.3 gives the turbulence intensity at a height of 75 m for a range of wind speeds and temperature differences. The figure shows that stability influences the turbulence intensity particularly at lower wind speeds. At higher wind speeds mechanical turbulence is dominant over convection.

3 Analysis of K13 database

3.1 Introduction

The K13 platform is an offshore gas production platform in the North Sea, situated at 53°13'04" N and 03°13'13" E, about 100 km off the coast at the height of the island Texel (see figure 3.1). Since 1978 meteorological measurements have been carried out on this platform. In 1982 it became part of the Measuring Network North Sea, which is jointly operated by RWS and KNMI [Witteveen, 1989]. This Network consists of eight meteorological stations in the North Sea and on the North Sea coast (see also figure 3.1; North Cormorant and AUK Alpha are not shown, these stations are located much further to the North). The measurements from this Network are mainly used for synoptic purposes, but are also stored on magnetic tape for later use.

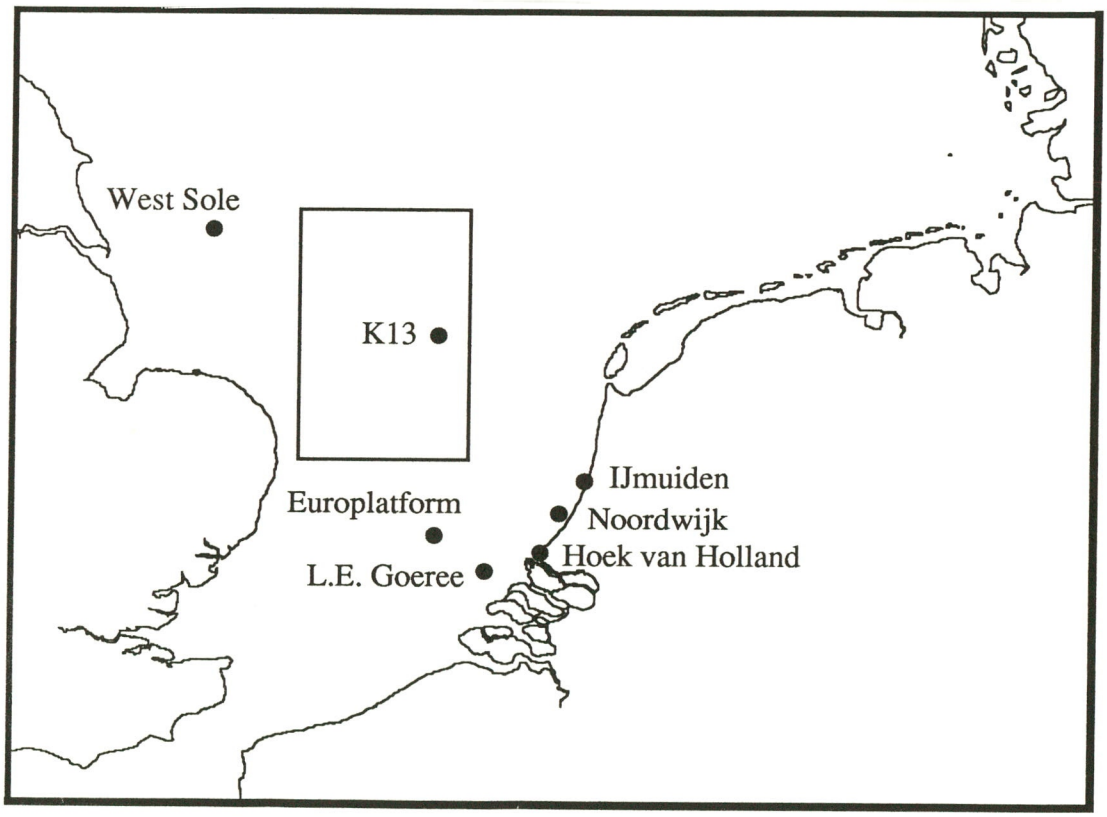

Figure 3.1 Overview of meteorological stations used in the Measuring Network North Sea (see also Witteveen et al., [1989]). Also shown is the area from which the seawater temperature database originates and the position of West Sole.

3.2 K13 platform

A side view of the K13 platform is shown in figure 3.2. The wind speed measurements are carried out using two anemometers, which are mounted on a lattice tower. The height of the anemometers is 74.9 m above MSL (= Mean Sea Level), or 73.8 m above LAT (= Lowest Astronomical Tide). Although two anemometers are present, only one is used for the actual measurements, while the other serves as a back-up in cases of failure. From the data it is not possible to determine which anemometer has been used. The height of the temperature sensor was 24 m above MSL. The wind direction is measured at the same height as the wind speed.

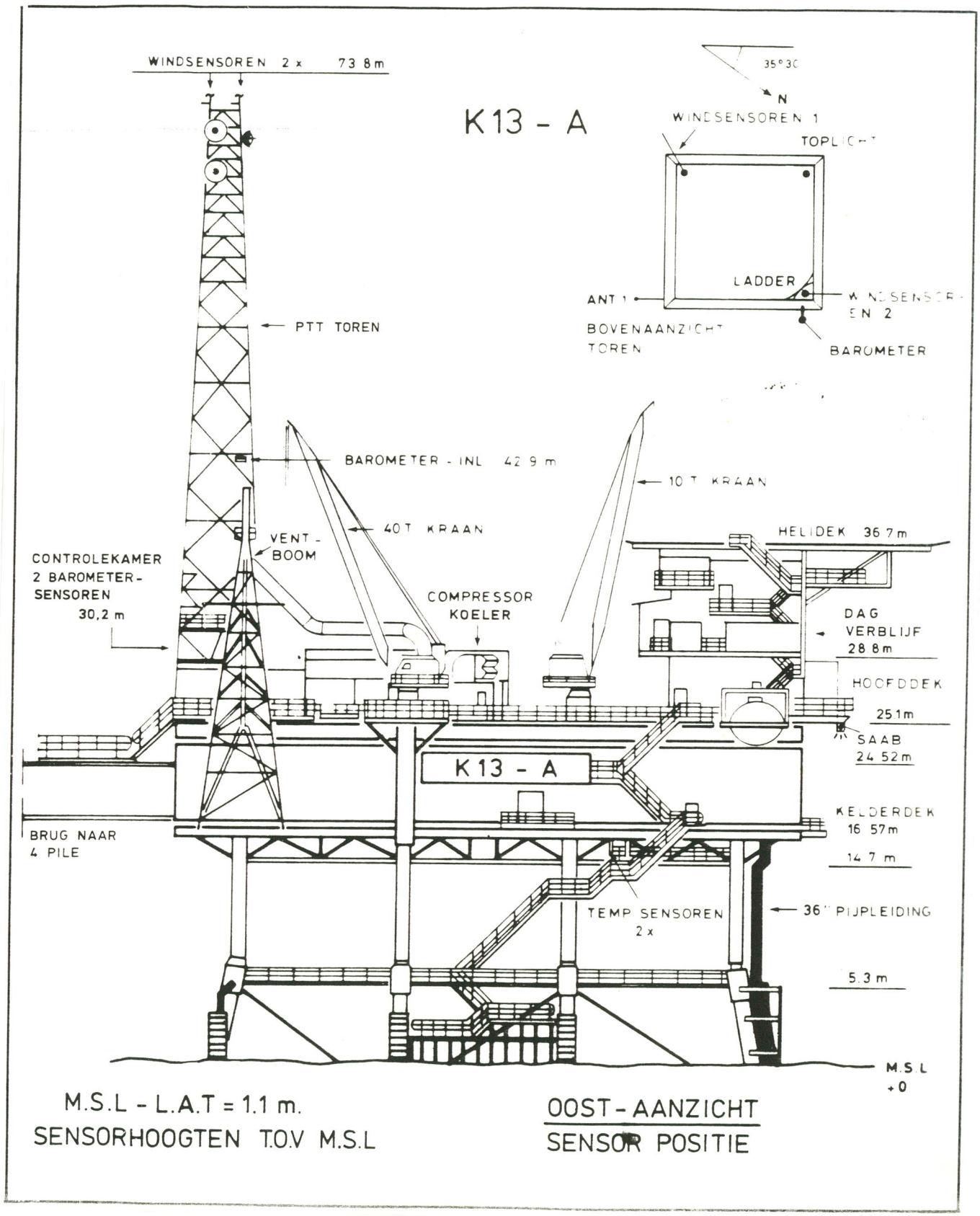

Figure 3.2 Side view of the K13 platform [Witteveen et al., 1989].

3.3 K13 database

The database obtained from KNMI contains measurements from the years 1982-1989. It consists of hourly records of the following quantities:

- 10-minute wind speed (in 0.5 m/s, average of the last 10 minutes before the hour);
- 1-hour wind speed (in 0.5 m/s);
- 10-minute (scalar) wind direction (in tens of °);
- air temperature (in 0.1°C);
- air pressure (in 0.1 mbar).The data from the Measuring Network North Sea are used by KNMI and others for synoptic purposes. Therefore a quality check is carried out by KNMI to eliminate obvious errors and to check the internal consistency of the data.

Although the tower is much higher than the other obstacles on the platform such as the cranes, for some wind directions the wind flow is still distorted and the wind speed measurements are not quite correct. These distortions have been studied by putting a scale model of the platform in a wind tunnel [Vermeulen et al., 1985]. The results show that in the directions between 340° and 80°, and in a very narrow sector around 240°, the wind speed measurements are distorted, between -4% and +9%. Because the distortions are limited, and because the distortions are different for the two anemometers and it is not known which one has been used, no corrections were applied to the data.

3.4 Seawater temperatures

3.4.1 Introduction

To determine the stability conditions above sea, the seawater temperature (measured at the surface) is needed. Because seawater temperatures are not measured at the K13 platform, these had to be obtained from another source. This source was a database consisting of measurements carried out by Voluntary Observing Ships. Data from these ships are collected by KNMI and subjected to a quality control programme [Korevaar, 1989].

3.4.2 Description database Voluntary Observing Ships

A database containing a selection of 6366 of these recorded measurements was obtained from KNMI. The records consisted of measurements made at random times of the day (usually standard times: 00, 06, 12 and 18 hours GMT), and from random positions, between 52.5°N and 53.9°N, and between 2.0°E and 3.9°E (this represents a rectangular area of about 160 km by 125 km around the K13 platform, also shown figure 3.1), all from the period 1982-1989. Each record contained the following elements:

- date and time;
- position in °N and °E;
- air and seawater temperature (in 0.1°C);
- wind speed and wind direction.

Because seawater temperatures do not vary on a timescale of a day, this database is sufficient for the purposes of this project. The processing of the data before use in the analyses is described in section 3.5.7.

3.5 Results

3.5.1 Availability of data, mean wind speeds and interannual variations

The first step in analysing the wind speed data is to determine the availability of data: i.e. the percentage of hours in a period for which a measurement has been given. In the hourly records the absence of a measurement was denoted by KNMI with X's. The availability of the 10-minute wind speeds and the 1-hour wind speeds is shown in table 3.1. In this table the annual mean wind speeds of each year are also shown, as well as the overall mean wind speed over the whole period of 8 years.

Table 3.1 Annual mean wind speeds and availabilities at K13 (1982-1989)

Year	10-minute wind speed		1-hour wind speed	
	Availability of data %	annual mean [m/s]	Availability of data %	annual mean [m/s]
1982	94.9	8.85	0.0	-
1983	99.3	7.74	87.6	7.61
1984	99.2	7.55	99.5	7.62
1985	96.0	9.08	96.5	9.40
1986	95.9	10.24	26.4	11.31
1987	97.4	9.08	56.0	9.65
1988	98.2	10.04	68.6	10.40
1989	95.7	9.46	83.6	9.70
1982-1989	97.1	9.00	64.8	9.06

From this table it can be seen that in 1982 there were no 1-hour wind speed data at all, and that in general the availability of 10-minute wind speeds is higher, especially in the years 1986-1988. It was also concluded that the periods when no 10-minute wind speeds were available, are scattered over the year and in the order of several hours. The fact that the overall mean wind speeds are nearly equal, is

more or less coincidental, given the fact that there are no 1-hour wind speeds in 1982. However, because the 10-minute wind speed in 1982 is very close to the overall mean wind speed, the overall mean is not much affected if 1982 is left out.

Because of the higher availability of the 10-minute wind speeds and because no new insight could be gained from the 1-hour wind speeds, the 10-minute wind speeds have been used in all further analyses.

From the table it can be seen that the annual variations for the 10-minute wind speeds are between +14% and -16% from the overall mean wind speed. This is high compared to variations presented by Wieringa and Rijkoort [1983] for land stations over a period of 30 years.

3.5.2 Annual courses

The next interesting feature is the annual course of the wind speed. The annual course shows the variation of the monthly mean wind speeds. In figure 3.3 the annual course for the 10-minute wind speed for the period 1982-1989 is shown, together with the average over all years.

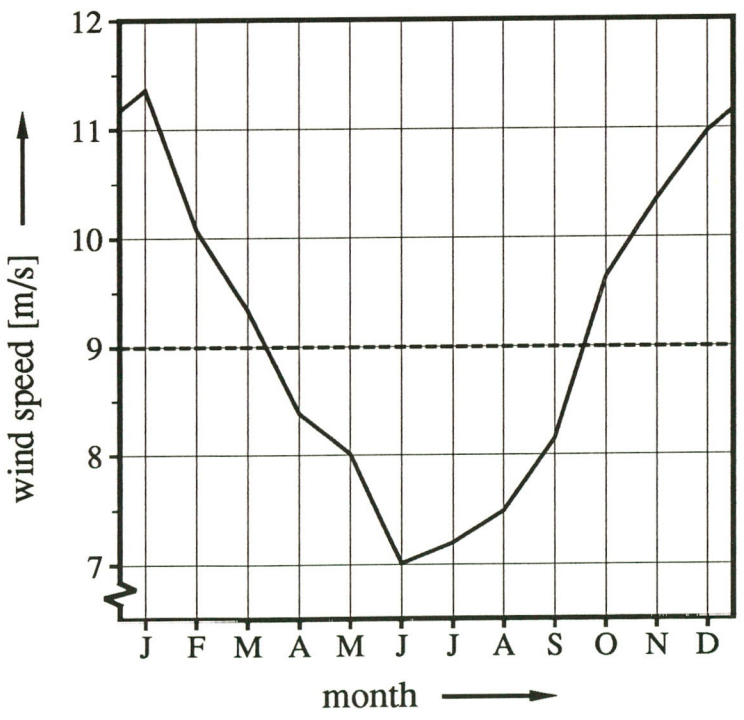

Figure 3.3 Annual course of the 10-minute wind speed at K13 (1982-1989) (solid line), together with the average over all years (dashed line).

As can be seen in figure 3.3, the seasonal effect is larger than above land (see e.g. Wieringa and Rijkoort [1983]). The monthly means deviate between +26% and -22% from the annual mean. Generally, the global pressure distribution causes higher wind speeds in winter than in summer. This is true both above land and above sea. However, above sea this effect is enhanced due to the seasonal variation of stability. This is caused by the following: seawater has a large heat capacity; the seawater warms and cools gradually during the months by vertical mixing; in autumn months (when the air is already cold and the seawater still warm), this results in unstable conditions, which means that high wind speeds at greater heights are transferred to lower heights; in spring months (when the air can already be warm and the seawater is still cold) this results in stable conditions, which means that at the surface just above the earth's surface the wind speeds are low.

3.5.3 Diurnal courses

The diurnal course shows how the wind speeds vary from hour to hour during the day. In figure 3.4 the diurnal course of the 10-minute wind speed for the period 1982-1989 is shown, together with the average over all years.

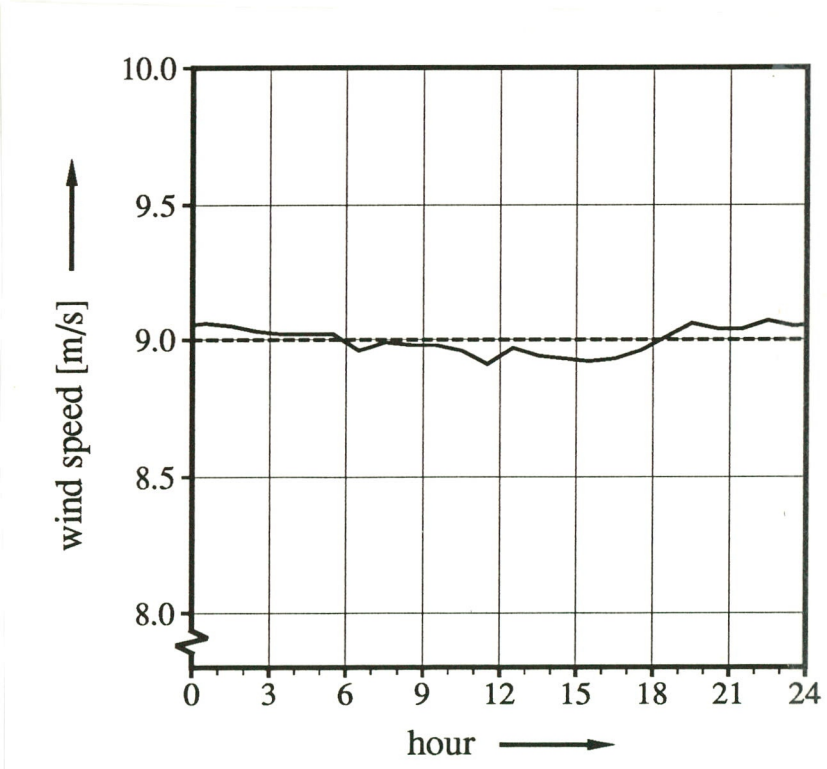

Figure 3.4 Diurnal course of the 10-minute wind speed at K13 (1982-1989) (solid line), together with the average over all years (dashed line).

From this figure it can be concluded that there is no mean diurnal cycle in the mean wind speed. This conclusion remains valid when looking at the diurnal

course averaged over any one month, regardless of the season. This can be understood as follows: the diurnal course in wind speed on land is caused by warming and cooling of the earth's surface, which generally results in stable conditions during the night and unstable conditions during the day. Above sea this effect does not occur due to the large heat capacity of the sea. There is no difference in the temperature profile between day and night, and therefore no diurnal variation in stability.

3.5.4 Frequency distributions and Weibull parameters

The frequency distribution of the wind speed has been made by determining the occurrence of measured wind speeds in 0.5 m/s intervals, because the database contains wind speeds in 0.5 m/s. Usually, intervals of 1 m/s are chosen for this purpose. The result is shown in figure 3.5.

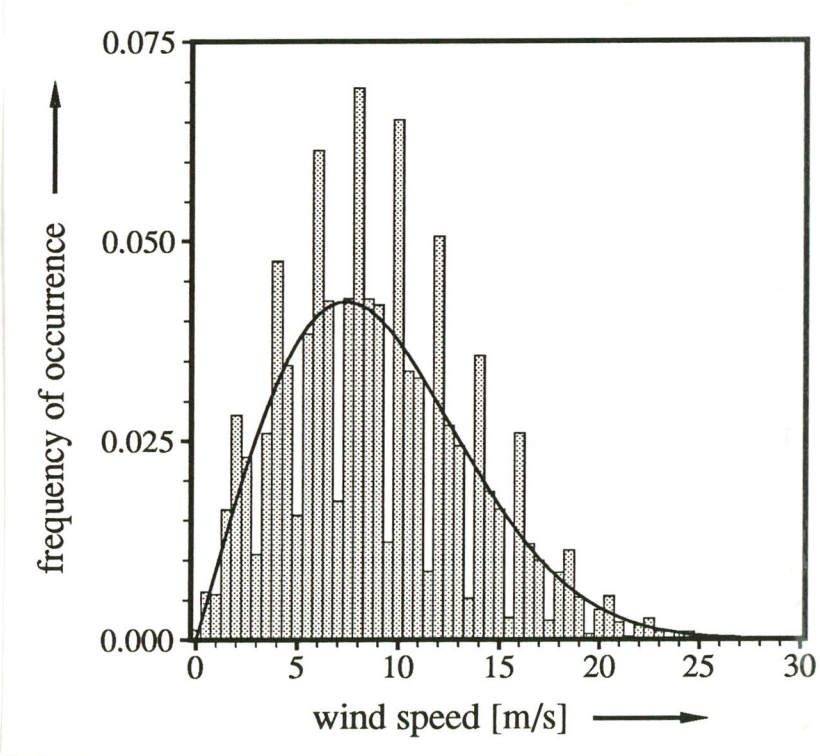

Figure 3.5 Frequency distribution of the 10-minute wind speeds at K13 (1982-1989). The solid line denotes the theoretical Weibull distribution with k = 2.04 and a = 10.25 m/s.

It can be seen that something peculiar must have happened: in some intervals the frequency of occurrence is evidently too low, while in others this seems to be compensated by a value that is evidently too high. To explain this anomaly KNMI and Rijkswaterstaat have been consulted, but it has not (yet) been possible to trace the origin of this behaviour. It appears to be some round-off error, because the

original anemometer signal in 0.025 m/s is transformed to another height, and also transformed into knots, and then corrected back to the original height and in 0.5 m/s intervals, before being stored for later use. This rather elaborate procedure is prone to computing errors like this. However, it does not seem to affect the analysis too much, as can be seen from table 3.1 for example. In this table the mean 10-minute wind speeds are compared to the mean 1-hour wind speeds, which do not exhibit this phenomenon. Other analyses of 1-hour wind speeds which are not presented here, also show no significant difference with 10-minute wind speeds. It is therefore decided to continue using the data like before.

Wieringa and Rijkoort [1983] have shown that wind speed frequency distributions can be described quite accurately by the two parameter Weibull distribution function [Wieringa and Rijkoort, 1983]:

with: f(U) probability that the wind speeds exceeds U
k shape factor, representing the 'skewness'

$$f(U) = \frac{k}{a}\left(\frac{U}{a}\right)^{k-1} e^{-\left(\frac{U}{a}\right)k} \qquad (5.1)$$

a scale factor

By using the Linear Least Squares method [Wieringa and Rijkoort, 1983], the two Weibull parameters k and a were calculated. From the values of k and a it is also possible to calculate the average value U_{mean} theoretically. Comparison of the actual mean and the calculated U_{mean} gives an indication how well the fit describes the frequency distribution. The results of these calculations are shown in table 3.2. The theoretical distribution function is denoted in figure 3.5 with the solid line.

Table 3.2 Weibull parameters of the wind speed frequency distribution at K13 (1982-1989)

	k	a	U_{mean}
10-minute wind speed	2.04	10.25 m/s	9.09 m/s

From this table it can be seen that the theoretically calculated mean wind speed deviates by no more than 0.1 m/s from the actual mean wind speed of 9.00 m/s (see table 3.1), so the Weibull distribution function describes the wind speed distribution well in this respect, despite the artefact in the data described previously.

3.5.5 Results by wind direction

It is interesting to look at the distribution of wind speeds by wind direction, especially for wind energy purposes, e.g. for the direction of placement of wind turbine clusters. For this purpose the wind directions have been transformed from tens of degrees into 12 sectors of 30°, where sector 1 represents the sector around the north, sector 2 the sector from 15° to 45° etc. This is common practice in wind energy applications.

The results of this analysis are shown in table 3.3. In this table the 10-minute wind speed in each sector is shown, but also the frequency of occurrence of each wind direction as a percentage of the time.

Table 3.3 Mean wind speeds and frequencies of occurrence by wind sector at K13 (1982-1989)

sector	frequency of occurrence %	wind speed [m/s]
1	6.1	7.55
2	6.3	7.43
3	5.6	8.44
4	6.6	8.86
5	5.2	7.54
6	5.5	7.90
7	8.4	9.08
8	14.2	10.47
9	13.6	9.95
10	11.6	10.06
11	8.5	8.65
12	7.8	7.99

From this table it can be seen that in the southwesterly direction (sectors 7-10) not only the mean wind speed is the highest, but that the frequency of occurrence is also the highest: 47.8%, or nearly half the time in only one third of the wind rose.

3.5.6 Statistics of temperatures

In general, the stability conditions depend on the temperature difference of air and seawater and the wind speed. In situations with high wind speeds thermal effects are negligible compared to mechanical effects, and the temperatures are not so important. At low wind speeds, however, thermal effects do become important for stability. If the sea is relatively warm compared to the air above it, the air is warmed from the bottom up. Warm air rises, and this results in vertical mixing of the air, or in other words, in an unstable condition. If, on the other hand, relatively warm air passes over a cold sea, then little or no vertical mixing of air will occur and this results in a stable condition. Therefore, the statistics of the temperatures of air and seawater are interesting for studying stability.

3.5.7 Processing of seawater temperature data

Before it was possible to use the seawater temperature database together with the K13 database, the data had to be processed.

First daily means of the seawater temperatures were calculated, regardless of the number of measurements available, of the position of the ship or of the time of day. In this way values were obtained for the daily mean seawater temperature of about 80% of all days (excluding 1989). For the year 1989 only a few measurements were available, so 1989 was excluded from the analyses altogether. In figure 3.6 the results are shown for the year 1982 as an example.

Although the origin of the measurements is quite varied, and the number of measurements of which the daily means consist varies between 1 and 15, the scatter is surprisingly small. The first column in table 3.4 gives the calculated mean values of the seawater temperature for each year, and the mean value calculated over all years. It can be concluded that the annual mean values of the seawater temperature differ between +9% to -5% from the overall mean during the period 1982-1988.

The next step was to make a fit through the datapoints, mainly for two reasons. The first is that seawater temperatures were needed for all days of the year, so some kind of interpolation was necessary anyway. The second is that, because at one location no large variation in seawater temperatures is to be expected, a fitting procedure would eliminate the scatter in the datapoints caused by the nature of the database. Looking at the points in figure 3.6 the following sine function was formulated:

$$Seawater\ temperature(day) = A + B \sin\left(\frac{2\pi}{T}(day - \phi)\right) \qquad (5.2)$$

with: day the number of the day in the year (1 January = 1, etc.);
A the annual mean seawater temperature (in °C);
B the maximum deviation of the mean (in °C);
T the period of the function (in this case chosen to be 365 or 366 days);
ϕ a phase difference (expressed in days).

Although this function has in fact four free parameters, a fixed value has been chosen for T. The result for A can be related to the actual mean seawater temperature as derived from the data. This gives an indication how well the fit describes the datapoints. The result of this fitting procedure is also shown for 1982 in figure 3.6.

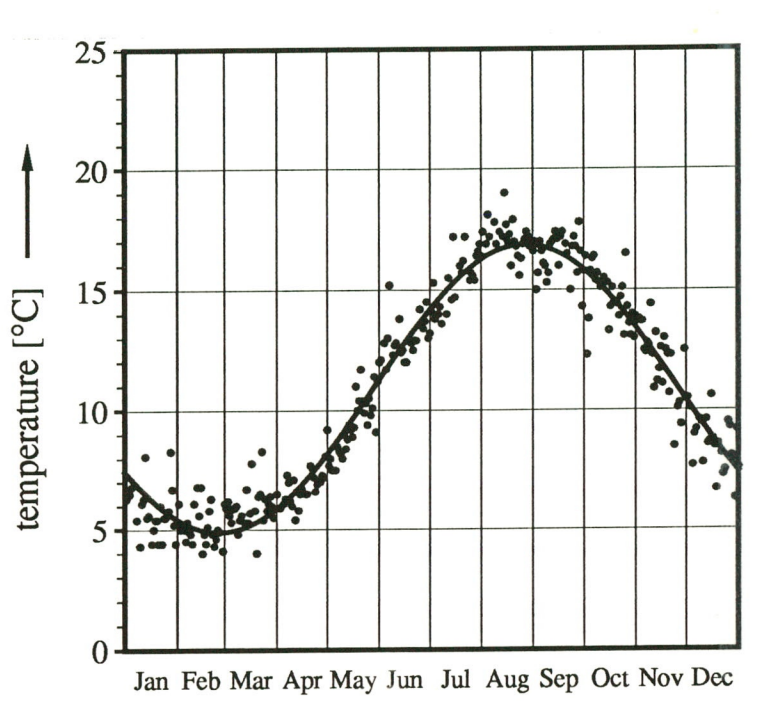

Figure 3.6 Daily means of seawater temperature and sine fit for the year 1982.

The resulting values of the calculated parameters of this fitting procedure for each year are shown in table 3.4. Also shown is the result when the fitting procedure is used for the data of all seven years together, with in this case T taken as a free parameter.

Table 3.4 Results of fitting seawater temperatures (T only calculated in last fit)

year	mean [°C]	A [°C]	B [°C]	T [days]	ϕ [days]
1982	10.84	10.91	6.00	365	147
1983	10.63	10.56	5.64	365	149
1984	10.40	10.47	5.34	366	157
1985	10.06	10.12	5.81	365	152
1986	9.87	9.87	6.05	365	150
1987	10.15	10.15	5.86	365	152
1988	11.29	11.29	5.07	366	150
1982-1988	10.34	10.40	5.68	365.6	149

From this table it can be concluded that the used fitting procedure gives good estimates for the annual means. For further processing of the K13 database these results were used.

For the assessment of the stability conditions it is quite interesting to look at the mean temperatures of air and seawater and their difference. This is especially so because the origin of both databases is different. In table 3.5 the annual means of these temperatures and their differences are shown. In this case the air temperatures measured at 24 m above MSL are corrected to a height of 2 m above MSL, using the dry adiabatic lapse rate (-0.01°C/m).

Table 3.5 Annual mean air and seawater temperatures and temperature differences at K13 (1982-1989)

year	air temperature [°C]	seawater temperature [°C]	temperature difference [°C]
1982	10.15	10.91	-0.85
1933	10.05	10.56	-0.44
1984	9.91	10.47	-0.61
1985	8.79	10.12	-1.23
1986	8.78	9.87	-1.08
1987	8.97	10.15	-1.19
1988	10.42	11.29	-0.86
1982-1988	9.59	10.48	-0.89

From this table it can be seen that the mean annual temperature differences are negative, which would mean that unstable conditions prevail at K13.

The annual means of the air temperature deviate between +16% and -10% from the overall mean, while for the sea temperature these variations are only between +8% and -6%. This was also to be expected, because of the difference in heat capacity between seawater and air. The seawater acts as a large heat buffer, with a relatively constant temperature compared to air.

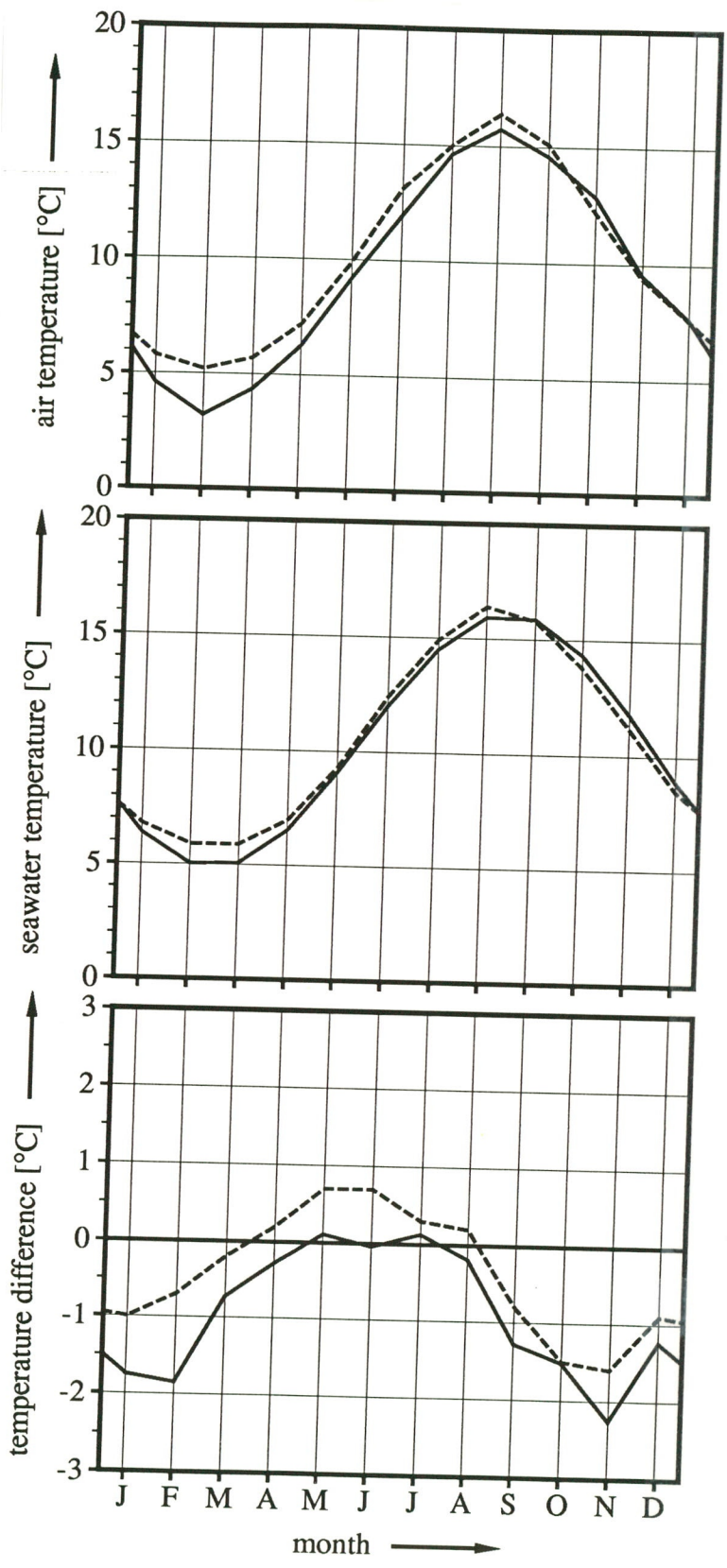

Figure 3.7a-c Annual courses of the air and seawater temperatures and the temperature difference, averaged over all years for K13 (1982-1988; solid lines) and for Area 20 (19771-1980; dashed lines) [Korevaar, 1989]

It is also interesting to look at the annual courses of air and sea water temperatures and their difference, which are shown in figure 3.7a-c. For comparison, results reported by Korevaar [1989] are also shown. These are the results from Voluntary Observing Ships, in Area 20. This is a rectangular area between 53°N and 54°N and 2°E and 4°E, which is almost identical to the area from which the database of the Voluntary Observing Ships has been compounded. Shown in the figure are the values for the period 1971-1980.
From figure 3.7c it can be concluded that there is a strong seasonal effect on the temperature difference. In spring and summer (from March to August) the temperature difference at K13 is either positive or slightly negative (between 0.13°C and -0.73°C), while in autumn and winter (from September to February) the temperature difference is strongly negative (between -1.24°C and -2.26°C).

It can also be concluded that, despite the difference in time periods, there is a great similarity in the annual courses of the temperatures and the temperature difference of K13 and Area 20. However, it must be kept in mind that the heights at which the air temperatures have been measured are not the same.

3.5.8 Statistics of stability

As was described in section 2.2, the value of the Obukhov length L represents the stability conditions within the PBL. In table 3.6 the frequency of occurrence for five stability classes is shown. The division into these classes has been done according to Van Wijk [1990]. For comparison, data reported by Van Wijk [1990] are presented in the table. These originate from a coastal station (IJmuiden-pier), when only wind speeds from sea directions have been taken into account. The wind speed data have been calculated with the diabatic wind profile from the measuring height of 18 m to a height of 70 m. The period considered was 4 years: 1973-1976.

Table 3.6 Statistics of stability conditions at K13 (1982-1988), compared to results of a coastal station IJmuiden-pier [Van Wijk, 1990].
[1])Values as found in this study for K13 (1982-1988).
[2])Values as reported by Van Wijk [1990] for IJmuiden-pier (1973-1976)

stability condition	value of L	U [m/s]		frequency of occurrence %	
		1)	2)	1)	2)
Very stable	0m<L<200m	7.20	6.35	10.3	17.7
Stable	200m≤L<1000m	11.57	11.06	13.3	18.4
Neutral	|L| ≥1000m	13.32	13.20	12.1	16.3
Unstable	-1000m<L≤-200m	12.37	12.17	16.2	17.4
Very unstable	-200m<L≤0m	7.86	6.97	48.1	30.0

From this table it can be seen that at K13 the conditions are very unstable or unstable 64.3% of the time, while they are very stable or stable only 23.6% of the time.

It can also be seen that with neutral conditions the mean wind speeds are the highest, and with very (un)stable conditions the lowest. This was to be expected: at high wind speeds the influence of thermal turbulence is negligible compared to the mechanical turbulence, while at low wind speeds the effect of thermal turbulence becomes important.

The table also shows a similarity in behaviour between K13 and IJmuiden-pier. At IJmuiden the overall stability has shifted somewhat towards more stable classes. However, still nearly half the time the conditions are (very) unstable. The resemblance in behaviour of the wind speeds is remarkable.

3.5.9 Roughness lengths

As was pointed out in section 2.2, for sea conditions the roughness length z_0 is no longer a constant but depends on the sea conditions, and therefore on the wind speed, as described by the Charnock relation. Calculation of the overall mean value of the roughness length resulted in a value of $z_0 = 0.00017$ m. This value is in quite good agreement with the generally accepted mean value of the roughness length for sea conditions of 0.0002 m [Van Wijk, 1990].

As z_0 is proportional to u_*^2, it is expected that z_0 increases strongly with increasing wind speed. For wind speeds smaller than 4 m/s an average value of 0.00002 m was found, while for wind speeds greater than 16 m/s an average value of 0.00055 m was found.

3.5.10 Planetary boundary layer heights

An interesting feature to look at is the height h of the PBL, calculated using the formulations (2.5) and (2.6) given in section 2.3.1. Variations in the value of h depend on the stability of the PBL, or simply on the value of L. This means that there is no diurnal course, but that there is a seasonal effect on the annual course, as shown in figure 3.8.

In very stable conditions the situation sometimes occurs that the calculated value of h is lower than the measuring height of the wind speed. This would mean that the measured wind speed is essentially the same as the geostrophic wind speed (see also section 2.3.1). However, this means that Monin-Obukhov similarity theory is not valid at this height anymore. This phenomenon occurred in 3.8% of all hours during the period 1982-1988.

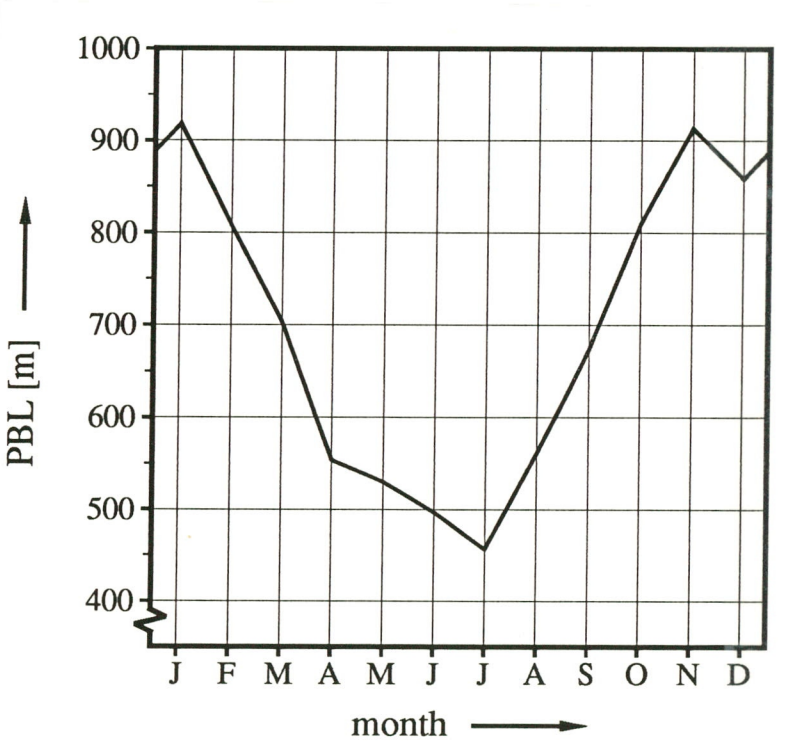

Figure 3.8 Annual course of the planetary boundary layer height at K13 (1982-1988).

It can be seen from this figure that in summer months (when (very) stable conditions occur the most) the PBL is thin and h becomes sometimes even lower than the measuring height. This aspect may well be relevant in wind turbine design.

3.5.11 Geostrophic wind speeds

As was pointed out in section 2.3.1, four different methods were used to calculate geostrophic wind speeds (equations (2.4), (2.7), (2.8) and (2.11)). Two of these ((2.4) and (2.8)) include stability effects, (2.7) is a neutral formulation. Expression (2.11) is based on pressure observations, and has been used by Børresen [1987] to compose a map for the North Sea of geostrophic wind speeds. For the database of K13 these expressions have been used to calculate the geostrophic wind speeds. The resulting overall mean geostrophic wind speeds are given in table 3.7, together with the Weibull parameters and the Weibull mean. This kind of detailed information is not available for the method based on pressure observations (2.11). Only mean wind speeds can thus be compared.

Table 3.7 Mean geostrophic wind speeds and Weibull parameters at K13 (1982-1988), and derived from Børresen [1987]

expression used	mean geostrophic wind speed	k	a	U_{mean}
(2.4)	10.16 m/s	1.75	11.21 m/s	9.98 m/s
(2.7)	10.53 m/s	1.78	11.56 m/s	10.29 m/s
(2.8)	10.38 m/s	1.78	11.46 m/s	10.20 m/s
(2.11)	10.5 m/s	-	-	-

From this table it can be concluded that the mean geostrophic wind speeds match reasonably well. That the neutral expression (2.7) gives a higher result, was to be expected from the fact that unstable conditions prevail at K13. Unstable conditions are characterized by strong vertical mixing, so the wind profile is relatively 'flat'. This means a relatively high wind speed at low heights, but also a relatively low wind speed at greater heights. A neutral formulation for the geostrophic wind speed will therefore give a higher mean. The rather coarse method to derive the geostrophic wind speed described by Børresen [1987], also matches well with the other, more refined, methods. However, this method does not provide any information concerning the frequency distribution or the Weibull parameters.

In Wieringa and Rijkoort [1983] geostrophic wind speeds have been calculated from measurements of land based meteorological stations. The calculations were done with expression (2.7), so stability effects were not taken into account. For locations on the North Sea coast and a few kilometres offshore a value of 13 m/s was found for the geostrophic wind speed. Going inland in southeasterly direction this value decreases to 9 m/s in the south of the province of Limburg. These results do not seem to match the values shown in table 3.7 at all, which range from 10.2 m/s to 10.5 m/s.

3.5.12 Wind profile results

In table 3.8 the annual mean wind speeds are shown, calculated at a height of 10 meters above MSL, using both the diabatic and the logarithmic wind profile, expression (2.3) and (2.1), respectively. As mentioned in section 3.5.10, the height of the PBL is sometimes lower than the measuring height. This poses a problem in the application of the diabatic wind profile because above the PBL Monin-Obukhov similarity theory can no longer be applied. This problem was solved by using an iterative procedure in which the height at which the measured wind speed is blowing, is lowered step by step until this height matches the then calculated value of h. This is a correct procedure if it is assumed that the geostrophic wind does not depend on height anymore.

Table 3.8 Annual mean wind speeds at 10 m at K13 (1982-1988), calculated with diabatic and the logarithmic wind profile

year	diabatic 10 m wind speed [m/s]	logarithmic 10 m wind speed [m/s]
1982	7.64	7.51
1983	6.64	6.58
1984	6.53	6.42
1985	7.90	7.69
1986	8.75	8.66
1987	7.66	7.68
1988	8.94	8.48
1982-1988	7.66	7.57

It can be seen that the influence of stability on the annual means is rather small. The difference between the overall means is 0.09 m/s (1%).

The relative interannual variations are the same as in the case of the measured wind speeds at 74.9 m shown in table 3.1: between +14% and -16%.

The Weibull k factor has also been calculated for the period 1982-1988 of the diabatically calculated wind speeds at 10 m. The result was 2.06, which is close to the value of 2.04 for the measured wind speed at 74.9 m (see table 3.2).

For synoptic purposes, measured wind speeds at different heights are always corrected to a height of 10 meters by KNMI (see [Witteveen et al, 1989]). For simplicity one factor is being used, which is 1.298 in the case of the K13 measurements. From the results presented in tables 3.1 and 3.8 it follows that this factor lies between 1.17 and 1.18 for the diabatically calculated mean wind speed, and between 1.18 and 1.19 for the logarithmically calculated mean wind speed. It can be concluded that in synoptic applications the mean wind speed at sea is underestimated.

Korevaar [1989] has processed the wind speed data into median wind speeds. The median wind speed is the wind speed that divides the frequency distribution in two halves with equal surfaces: half of the wind speeds is higher than the median wind speeds, and half is lower.

The median wind speed can also be calculated theoretically from the Weibull parameters according to Wieringa and Rijkoort [1983]:

$$\langle U \rangle = a\,(ln2)^{\frac{1}{k}}$$

In table 3.9 the calculated median wind speeds at 10 m height for K13 are shown together with the median wind speeds given by Korevaar [1989] for Area 20:

Table 3.9 Monthly median wind speeds for Area 20 (1971-1980) [Korevaar, 1989], and for K13 (1982-1988), calculated diabatically at 10 m

month	median wind speeds Area 20 [m/s]	median 10 m wind speeds K13 [m/s]
January	7.2	8.89
February	5.7	7.81
March	6.7	7.16
April	7.2	6.24
May	6.7	6.22
June	5.1	5.48
July	6.2	5.35
August	5.1	5.63
September	7.2	6.51
October	8.8	7.40
November	9.3	8.49
December	9.8	9.04
Overall	6.7	7.01

From this table it can be seen that the annual course of the median wind speeds for Area 20 and for the 10 m wind speeds at K13 is quite similar.

4 Analysis of west sole database

4.1 Introduction

The West Sole wind measurement project started in June 1978 and measurements continued there until October 1988. The project was set up originally as a collaboration between British Marine Technology (BMT, then the National Maritime Institute), BP and the Department of Trade and Industry, primarily to try to improve the prediction of wind loads on offshore structures. Over the ten years the emphasis has changed, with the major interest now being the provision of wind data for offshore Wind Turbine Generators, and with financial support coming from the Department of Energy through ETSU, the Energy Technology Support Unit [Wills, 1989].

Due to problems of access to the platform many periods of data are missing. However, the dataset is particularly interesting because wind recordings were made at seven different heights and thus offers a rare opportunity to derive the wind profile over sea. Except mean properties of the wind a limited amount of recordings was made with a larger sampling rate. These data were used to obtain power spectra and coherence functions of the wind speed. Results of these fast measurements are reported separately in chapter 6.

The University of East Anglia have used two years (1983-1985) of the West Sole data to analyze the wind profile, stability and seasonal and diurnal courses. The results, however, are not published yet, but will be incorporated in a Ph.D. thesis.

4.2 Description West Sole database

4.2.1 West Sole platform

The West Sole "A" platform is the main platform in the West Sole gas field (52°43'13"N 01°09'00"E) near the British shore (see figure 4.1). It is a small jacket structure consisting of the main platform housing the accommodation module and helideck, and two satellite platforms connected by foot bridges, one to the west and one to the east. The eastern satellite platform carries the gas treatment plant and the radio tower. In the experiment the slender, open lattice radio tower was used to mount the wind measuring equipment. The water depth is about 25 m.

As can be seen from figure 4.1 the radio tower is well exposed to the south. To the north there is some disturbance from the gas treatment plant at the lower levels. The main disturbance comes from the main platform to the west, extending between 20 to 40 m above sea level.

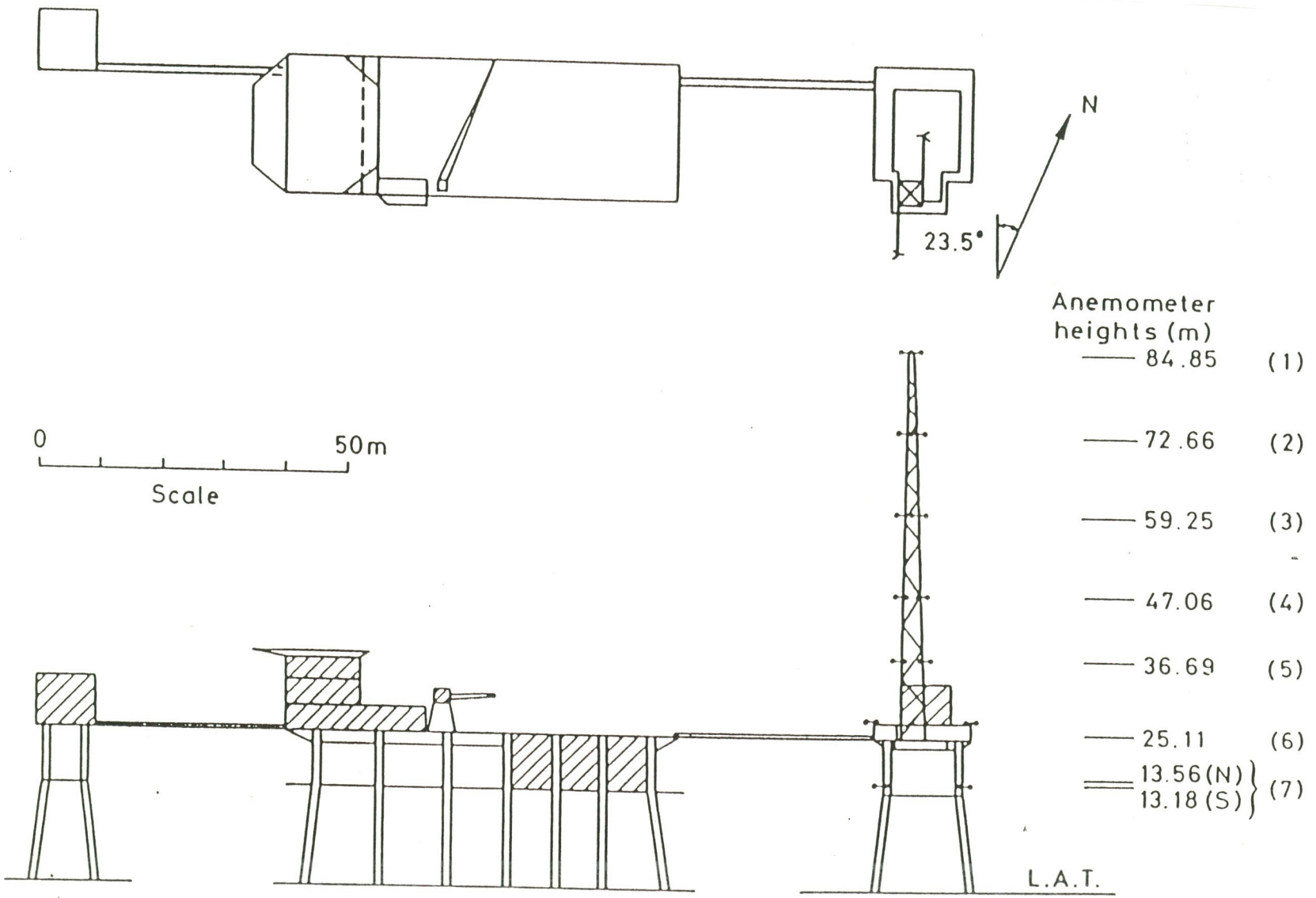

Figure 4.1 The West Sole "A" platform

4.2.2 Measuring equipment

Wind speed measurements were made on seven different levels using Porton cup anemometers with a distance constant of 5 meters. At each levels two cup anemometers were mounted to the radio tower through 3 meter long booms one to the north and one to the south. In this way always one of the anemometers was unobstructed to the wind.

Wind direction was recorded by means of a Porton wind vane mounted on top of the radio tower. The wind direction was read by means of a 4 bit Gray code giving the wind sensor a 22.5° resolution, centred on N, NNE, etc.

Two temperature sensors were used, one mounted on the tower top, the other one on the main-deck railing. In the present study the top-most temperature sensor has been used.

Wave heights were detected by means of a wave staff mounted on the north side of the main platform. This quantity was used in the BMT studies to correlate wave heights and wind speed data. We mention the wave staff for completeness as we do not analyze any wave data in the present study.

4.2.3 Signal processing and data-logging

All sensors were scanned at a rate of 2 Hz. Every 3 minutes averages of:
- temperature,
- wind speeds at 7 levels for north and south anemometers,
- rms-value of the wind speeds and
- wind direction

were stored on magnetic tape.
Moreover, for each anemometer the maximum 3-second wind speed in the 3 minutes period was recorded. The accuracy of the sensors was 1-2%, roughly.

The average wind direction was obtained in the following way. The Gray code was converted to a value between 1 and 16. The number of occurrences of each of these positions was stored during the three minute period. This distribution was converted to a mean wind direction by a process analogous to a Fourier transform. This process only works well when the wind direction fluctuations are sufficiently large during the 3-minute period. Otherwise, only values will be found corresponding to the sectors N, NNE etc. In section 4.4.4 we will show that this has been the case in the West Sole experiment.

During high-wind conditions, the system could switch to a rapid sampling mode, recording five samples per second from all seven anemometers on the windward side of the mast for a period of two hours. This enables the derivation of power spectra and coherence functions, which are treated in chapter 6.

Besides the sensor data a flag was recorded on the tape which reflected the status of the sensors. Any failure of the sensors would result in a flag being set.

4.3 Database and reduction of the dataset

4.3.1 Database

The West Sole database contains data over the period 1979 to 1989. For various reasons, more or less uninterrupted periods of recordings are available over 1983 and 1984 only (see figure 4.2). For the present study we have selected data which were recorded in the period from June 1983 to May 1984. The data were made available by BMT.

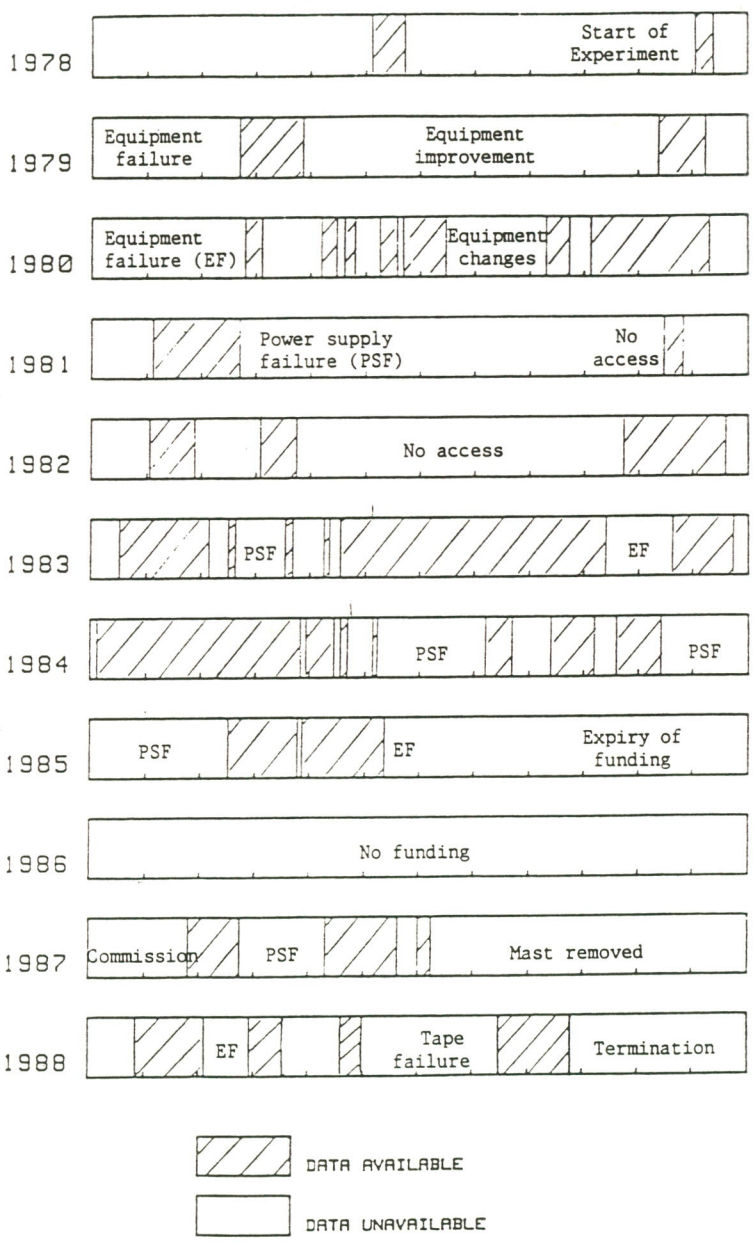

Figure 4.2 Overview of available data at West Sole.

The selected database contains the following entries:
- record count
- date and time of the recording
- flag
- wind speeds of 7 levels, for the north and south array
- turbulence intensity i.e. σ_U/U at 7 levels
- maximum 3-second wind speed at 7 levels
- wind direction
- air temperature at the top-most level (85 m height)
- seawater temperature

The flag contains information on:
- data discontinuity
- anemometer array to be selected (south or north)
- functioning of the anemometer

The sea surface temperature was not obtained by simultaneous measurement at West Sole but taken from the Meteorological Historical Sea Surface Temperature dataset. The values were means over a five-day period for the sea area 53.0°-53.9°N, 1.0°-1.9°E and the dataset is described in more detail in [Minhinick]

4.3.2 Data Reduction

The 3-minute values in the West Sole dataset have been converted to hourly average values of the wind speeds, the turbulence intensity, the wind direction and the temperatures. In this way the dataset is easier to handle and the results of the analysis can be compared to those of K13 directly. Further the maximum wind speed in the hour was determined by taking the maximum 3-second value in the observed hour.
The average hourly wind speed was written to the database whenever the number of 3-minute values in the hour exceeded 13. The value of the flag determined whether the north or south anemometer array was selected for the averaging process. The average wind direction was determined by linear superposition of the wind direction vectors of unit length and written to the database.

The original West Sole database contains the 3-minute turbulence intensity I,

$$I = \frac{\sigma_U}{U}$$

The conversion of the 3-minute turbulence intensity to an hourly average is not trivial. It is not sufficient to simply take the average of the 3-minute turbulence intensities.

We have used two methods to derive an hourly turbulence intensity.
Turbulence intensity I_3
The 3-minute values of $\sigma_U{}^2$ are averaged and the square-root is taken. The result is divided by the hourly mean wind speed in order to arrive at the turbulence intensity. Hence,

$$I_3 = \frac{\sqrt{AVG(\sigma_U 2)}}{AVG(U)} \qquad (4.1)$$

I_3 is characteristic for the turbulence intensity on a time-scale of the 3 minutes.

Turbulence intensity I_{60}
This is true turbulence intensity that would be found if a measuring period of 60 minutes was taken instead of 3 minutes. It is derived by calculating the total standard deviation of the wind speed during the hour (the square-root of the variance) divided by the hourly mean wind speed

$$I_{60} = \frac{\sigma_{U,hr}}{AVG(U)} \tag{4.2}$$

$\sigma_{U,hr}$ follows from the relation

$$\sigma^2_{U,hr} = \sigma^2(U) + AVG(\sigma_U 2) \tag{4.3}$$

$\sigma^2(U)$ is the variance of the 3-minute average wind speeds in the observed hour. The two right-hand terms have been stored in the data-base. This procedure yields the turbulence intensity, which is characteristic for the hourly time-scale.

4.4 Statistics hourly data

In this chapter we make an analysis of the available hourly wind speed data. The analysis is of limited value, since only less than a year of data is available. This is a too short period to make any profound climatological analysis of the West Sole location. However, as the measuring period of K13 and West Sole overlap we will compare the wind speed data of these wind measuring stations.

In the analysis we used measuring height 2 (at 73 m above LAT) as reference height. The wind speed at this height is denoted U_{73}. The reasons for this choice are, that the availability at height 2 is the highest, that height 2 is the most similar to the anemometer height at K13 and that at this height the influence of the tower on the wind flow is negligible.

4.4.1 Availability of data, mean wind speeds and interannual variations

In table 4.1 two different mean wind speeds at West Sole are shown: the mean using all available wind speed data at a particular height, and the mean using the hours during which wind speed data were available at all heights

Table 4.1 Mean wind speeds and availabilities at West Sole

Height [m]	Mean wind speed [m/s]1)	Availability %	Mean wind speed [m/s]2)	Availability %
85	10.1	43.0	10.9	25.7
73	10.0	67.1	10.9	25.7
59	9.8	65.9	10.4	25.7
47	9.4	62.3	10.3	25.7
37	9.5	28.9	9.5	25.7
25	8.8	66.0	9.1	25.7
13	8.3	66.1	9.0	25.7

1) mean calculated using all available wind speed data at each particular height
2) mean calculated using those hours during which wind speed data were available at all heights

It can be seen from table 4.1 that the average wind speeds are quite different, depending on the set of data used.

Table 4.2 depicts the Weibull parameters of the wind speed distribution at the seven measuring heights based on all the available wind speed data. Figure 4.3 gives the wind speed distribution for reference height 2.

Table 4.2 Weibull parameters at West Sole

Height [m]	scale factor a [m/s]	shape factor k
85	11.1	2.22
73	11.0	2.23
59	10.8	2.23
47	10.3	2.30
37	10.5	2.45
25	9.6	2.10
13	9.1	2.00

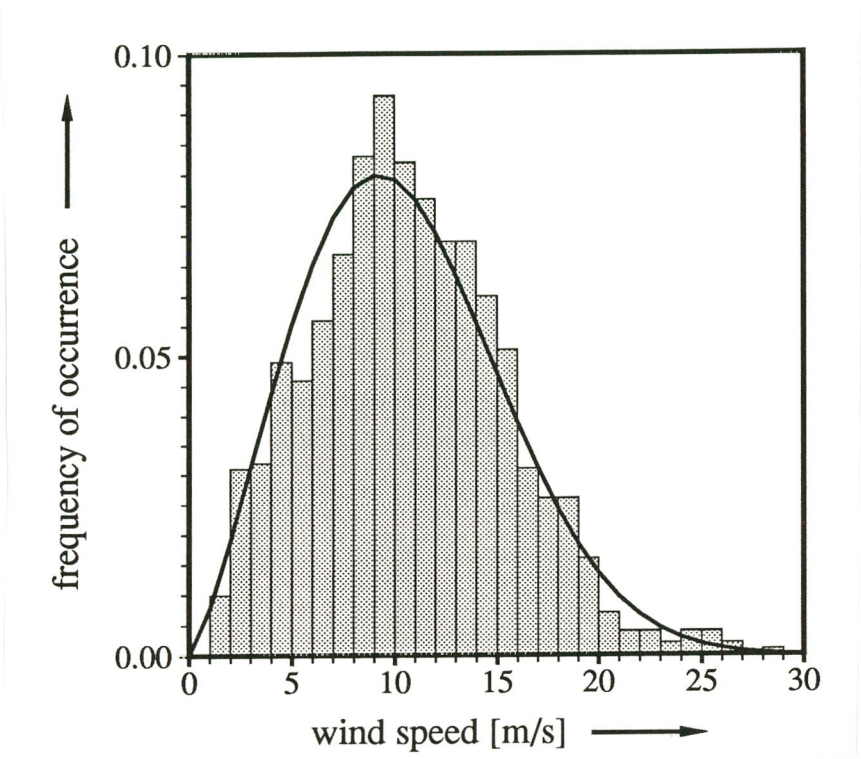

Figure 4.3 The wind speed distribution at reference height 2.

4.4.2 Diurnal course

Figure 4.4 shows the diurnal course of the wind speed at the reference height. The wind speed varies from 9.6 m/s at 1200 h GMT to 10.4 m/s around midnight. This means a variation of ±4% around the mean value.

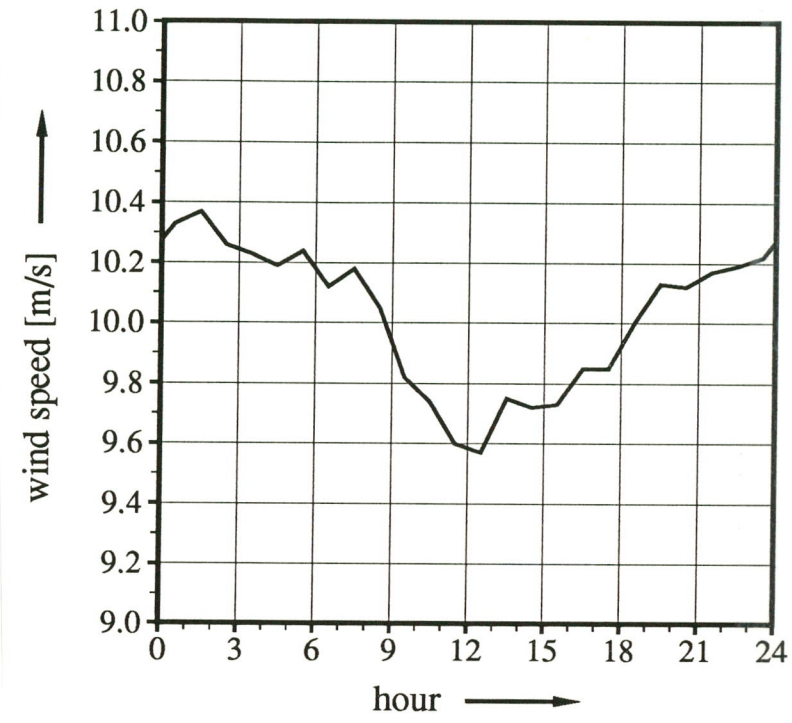

Figure 4.4 Diurnal variation of the wind speed at level 2.

When we compare this result with the result of the K13 platform we see that the diurnal variation at West Sole is larger than at K13.

4.4.3 Results by wind direction

Table 4.3 gives the frequency of occurrence and the mean wind speed per wind sector at level 2.

Table 4.3 Mean wind speeds and frequencies of occurrence by wind sector of 22.5° at West Sole (1983-1984)

sector	frequency %	wind speed [m/s]	sector	frequency %	wind speed [m/s]
1	6.1	8.76	9	3.4	9.87
2	5.6	8.07	10	3.9	10.36
3	6.1	7.71	11	7.7	11.91
4	3.9	6.76	12	6.2	11.97
5	2.2	7.62	13	4.9	12.74
6	2.8	9.51	14	4.7	12.05
7	2.9	9.40	15	3.3	10.35
8	3.1	9.84	16	1.4	9.96

Contrary to K13 we have analysed the data using 16 sectors of 22.5°. In this way the bins correspond to the Gray code of the wind direction sensor. Binning according to the same intervals as in the case of K13 would lead to erroneous results. This can be seen from figure 4.5, where we have depicted the frequency distribution of the wind directions with a resolution of 1 degree. The figure shows that high frequencies of occurrence at regular intervals of 22.5° are alternated by intervals with a very low frequency of occurrence. This discontinuous behaviour is clearly an artefact caused by the measuring and processing procedures used at West Sole. Using normal 30° intervals also causes an irregular pattern in the frequency distribution. The use of intervals of 22.5° has overcome this problem.

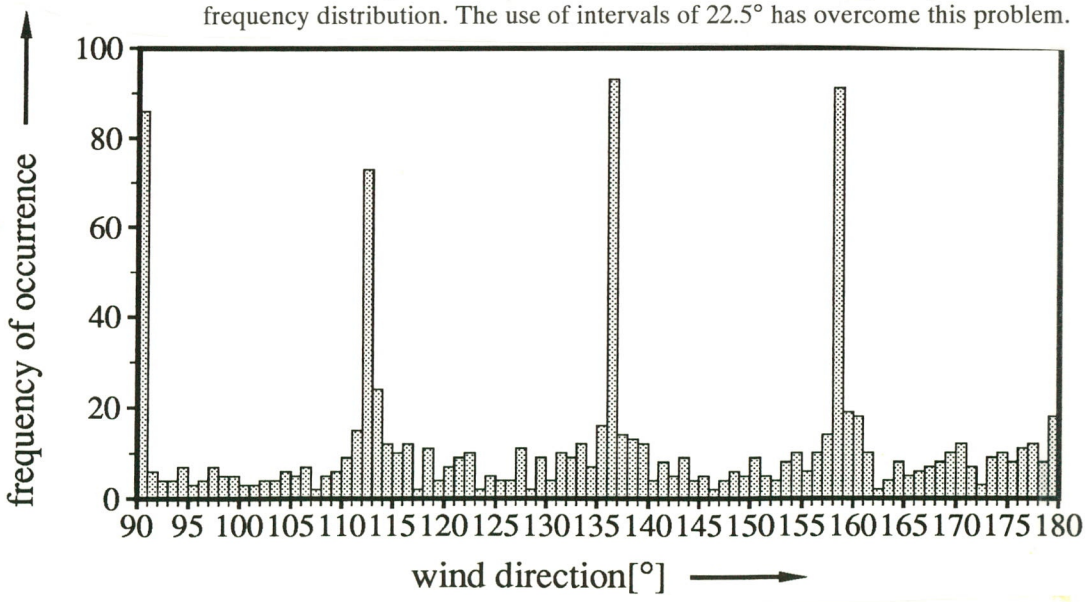

Figure 4.5 The distribution of wind directions at West Sole at level 2 depicted with 1° resolution.

4.4.4 Statistics of temperatures

At West Sole the air temperature has been measured at 85 m height. This temperature was transformed to the air temperature at 2 m height. As we have seen before no simultaneous measurements of the seawater temperature were made at West Sole. Instead use was made of the Met Office Historical Sea Surface Temperature Dataset. The average air temperature at West Sole was 10.1 °C and the seawater temperature was 9.1 °C.
Figure 4.6 gives the annual course for the air temperature and the seawater temperature. In figure 4.7 the annual course of the temperature difference is given. These figures show that throughout the year at West Sole the sea water temperature is higher than the air temperature. This do not seem to be realistic results, which are caused by the fact that a long term database was to used to derive the sea water temperature. This shows that in order to derive accurate temperature differences, it is essential to have available a dataset of sea- and air temperatures, which have been measured simultaneously.

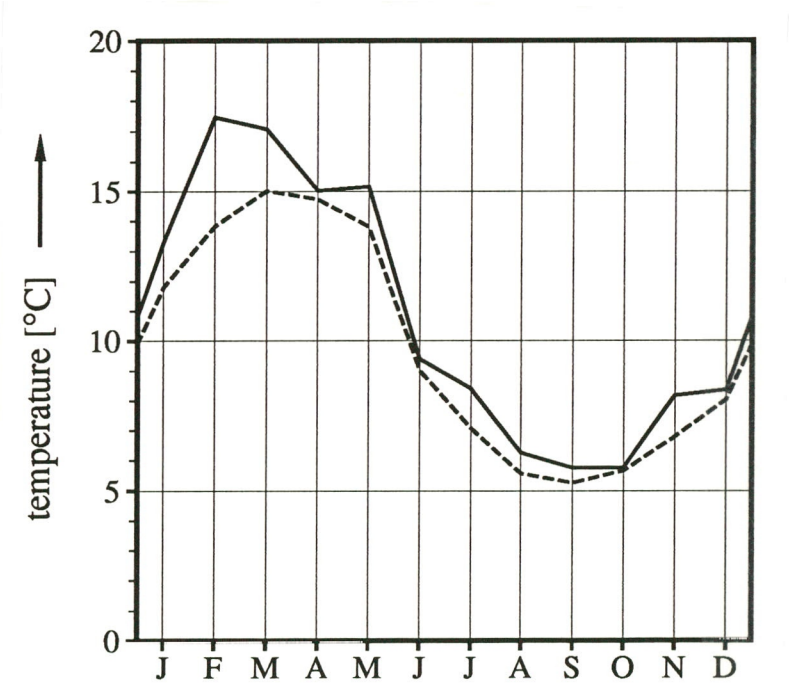

Figure 4.6 The annual course of sea water (dashed line) and air temperature (solid line) at West Sole.

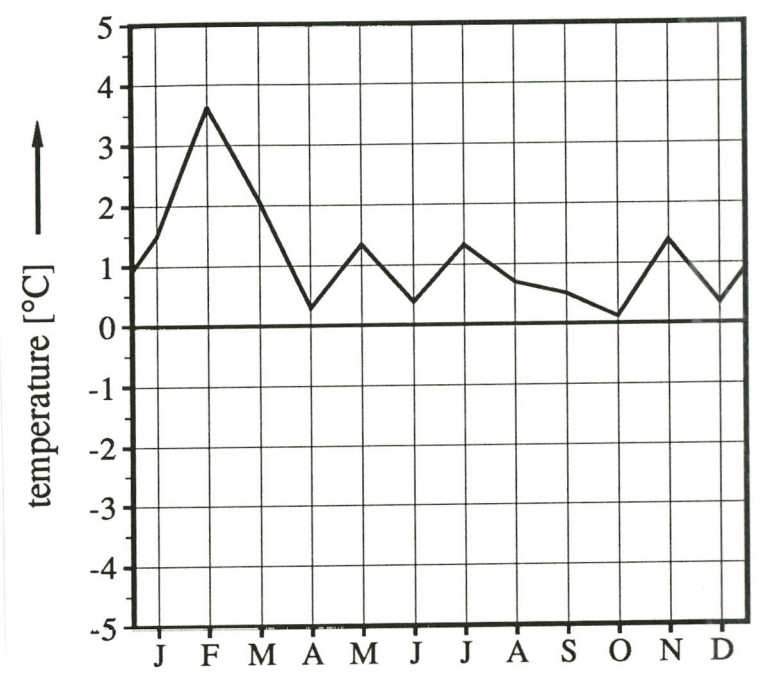

Figure 4.7 The annual course of the temperature difference at West Sole.

4.4.5 Statistics of stability

The stability conditions at West Sole have also been studied. In table 4.4 the results of this analysis are shown, where the wind speed at height 2 has been used as the reference wind speed.

Table 4.4 Statistics of stability conditions at West Sole

Stability condition	Value of L	Frequency of occurrence
Very stable	0 m<L<200 m	38.2%
Stable	200 m≤L<1000 m	18.7%
Neutral	|L|≥1000 m	14.2%
Unstable	-1000<L≤-200 m	11.5%
Very unstable	-200 m<L≤0 m	17.4%

It should be noted that the stability results have been obtained using the historical temperature data and hence the results are unreliable. This is also clear when the results are compared with the stability results of K13.

4.5 Wind profile calculations

4.5.1 Introduction

In the previous sections it has been shown that the temperature difference at West Sole cannot be used for correctly calculating the diabatic wind profile. Because the West Sole database is unique in that it offers the opportunity to make such comparisons, it is still interesting to compare the measured wind profile with the calculated diabatic and logarithmic wind profiles, despite this problem. However, we do not pose too much significance in the results.

4.5.2 Wind speeds

In section 2.2 two wind profiles have been described: the logarithmic wind profile (2.1) and the diabatic wind profile (2.3). The logarithmic wind profile only needs the wind speed at one height and a (constant) roughness length. The diabatic wind profile includes stability effects, for which the temperatures of air and seawater are needed also. In this case the roughness length is variable and is calculated as well.

In figure 4.8 the measured wind speeds are shown (squares), but only for the hours during which all wind speeds were available. Also the two calculated wind profiles are shown, using the wind speed at height 2 (72.66 m) as the reference wind speed. The solid line denotes the diabatic wind profile calculated according to equation (2.3), the dashed line denotes the logarithmic wind profile calculated according to equation (2.1).

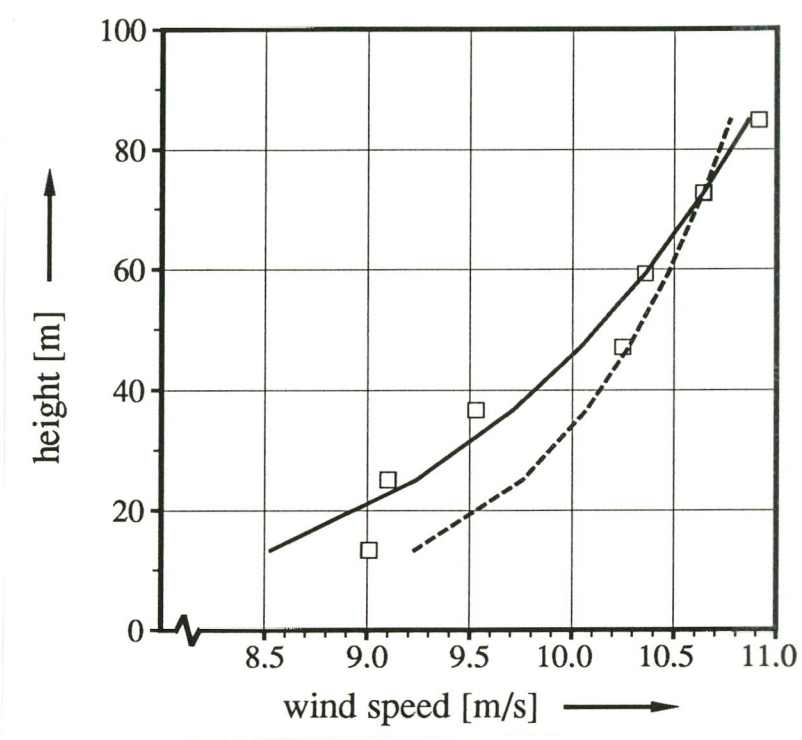

Figure 4.8 Observed wind speeds (squares), together with diabatic wind profile (solid line) and logarithmic wind profile (dashed line).

Qualitatively, it can be seen that the diabatic wind profile fits the observed wind speeds better than the logarithmic wind profile. Quantitatively, this can be expressed by calculating the root-mean-squares, or rms-values. The definition of the rms-value is given by this expression:

$$rms = \frac{\sqrt{\sum_i (V_{model,i} - V_{observed,i})^2}}{N} \qquad (4.4)$$

with N the number of points used. In this case the rms-value is expressed in m/s, and can be interpreted as the mean error in the model prediction.

In table 4.5 the rms-values are shown for each height, both for the diabatic and the logarithmic wind profile.

Table 4.5 Rms-values for calculated diabatic and logarithmic wind profiles

height [m]	rms diabatic [m/s]	rms logarithmic [m/s]
84.85	0.266	0.295
59.25	0.476	0.492
47.06	0.468	0.543
36.69	0.698	1.042
25.11	0.987	1.302
13.34	1.621	1.902

As can be expected, the rms-values increase as the difference in height increases. The rms-values for the diabatic wind profile are somewhat lower than the for the logarithmic wind profile, which indicates that the diabatic wind profile gives a better fit.

4.5.3 Stability

After having looked at the overall performance of the diabatic wind profile compared with the logarithmic wind profile, the same comparison is made for different stability conditions. In figures 4.9a-e, again the observed wind speeds are shown together with the diabatic and logarithmic wind profiles, for very unstable, unstable, neutral, stable and very unstable conditions, respectively.

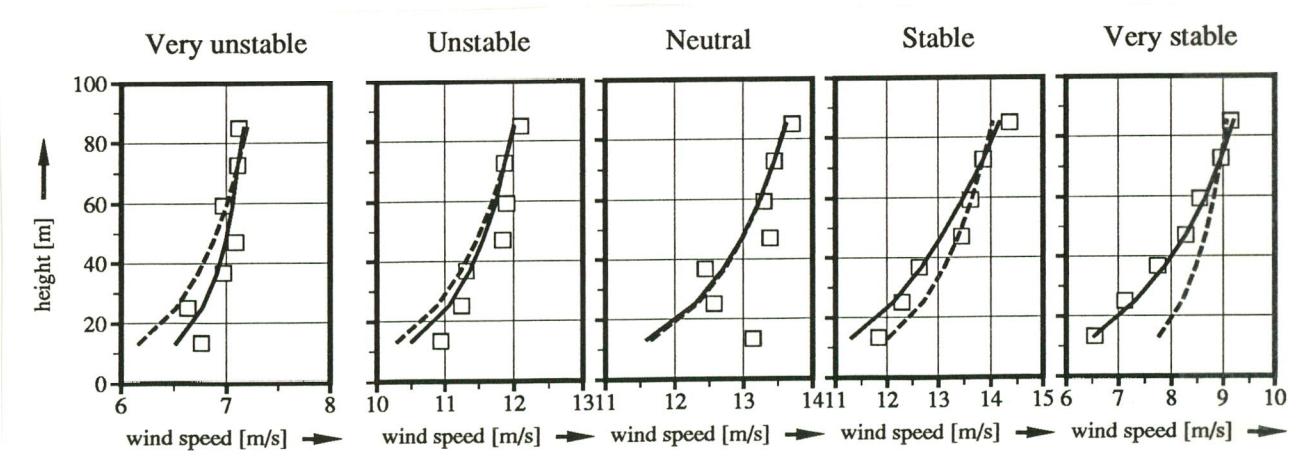

Figure 4.9a-e Observed wind speeds (squares), together with diabatic wind profiles (solid lines) and logarithmic wind profiles (dashed lines) for different stability conditions.

It can be seen that the stability conditions which occur the least number of hours (very unstable, unstable and neutral), show the most scatter in the data points (Fig 4.9a-c). For very stable conditions the scatter is the least. In this case especially, the diabatic wind profile fits the measured wind speeds almost perfectly. However, the results are not sufficiently consistent to be able to draw any well-founded conclusions with regard to the validity of the diabatic wind profile.

4.5.4 Geostrophic wind

As described in section 2.3.1, the geostrophic wind speeds at West Sole are calculated. The results are shown in table 4.6.

Table 4.6 Mean geostrophic wind speeds and Weibull parameters at West Sole calculated using the reference wind speed, and derived from Børresen [1987]

expression used	mean geostrophic wind speed	k	a	U_{mean}
(2.4)	12.03 m/s	1.93	12.82 m/s	11.37 m/s
(2.7)	11.99 m/s	2.08	13.43 m/s	11.90 m/s
(2.8)	12.01 m/s	1.90	12.79 m/s	11.35 m/s
(2.11)	10.7 m/s	-	-	-

From the table it can be seen that the three calculated mean geostrophic wind speeds match very well. However, the fourth method based on pressure observations, does not match the other three at all. The calculated values are consistently higher. This result also leads us to the conclusion that the wind speeds measured at West Sole are too high.

4.6 Statistics turbulence intensity

4.6.1 Data reduction and analysis of turbulence intensity

The 3-minute turbulence data were converted into two distinct average turbulence levels I_3 and I_{60} as was described in section 4.2.2. I_{60} takes into account the full turbulent fluctuations in the observed hour, while I_3 represents the average turbulence level in a 3-minute period corresponding to the hourly mean wind speed.

In order to find the relations between turbulence intensity and average wind speed for all heights the I_3 and I_{60} have been binned with respect to the average hourly wind speed at level 2. The bin width used was 1 m/s. Wind directions between

247° and 271° have been discarded as in this region the turbulence levels were contaminated by structure induced disturbances. Figure 4.10 gives the results of the analysis. For low wind speeds the turbulence intensity I_{60} is close to 0.15, For higher wind speeds first the intensity level drops and then increases gradually to a value of approximately 0.08.

The figure also depicts the theoretically expected levels at the various heights according to section 2.4.
For the levels 1 to 5 and wind speeds above 10 m/s the theoretically predicted and experimentally found values clearly coincide. The turbulence intensities of the two bottom-most levels, levels 6 and 7 show higher turbulence intensities levels than predicted. Probably, at these levels the influence of the tower is more pronounced.

For low wind speeds the experimental values differ markedly from the theoretical values. Remember that the theoretical curve is only valid for a neutral atmosphere. Apparently, the turbulence intensities at low wind speeds correspond to a non-neutral stability of the atmosphere at the lower wind speeds. Therefore, in the next section the turbulence intensity data have been analysed with respect to stability.

However, we may conclude that for wind speeds higher than 10 m/s the predictions based on the Charnock relation and the logarithmic profile are in good agreement with the experimental data.

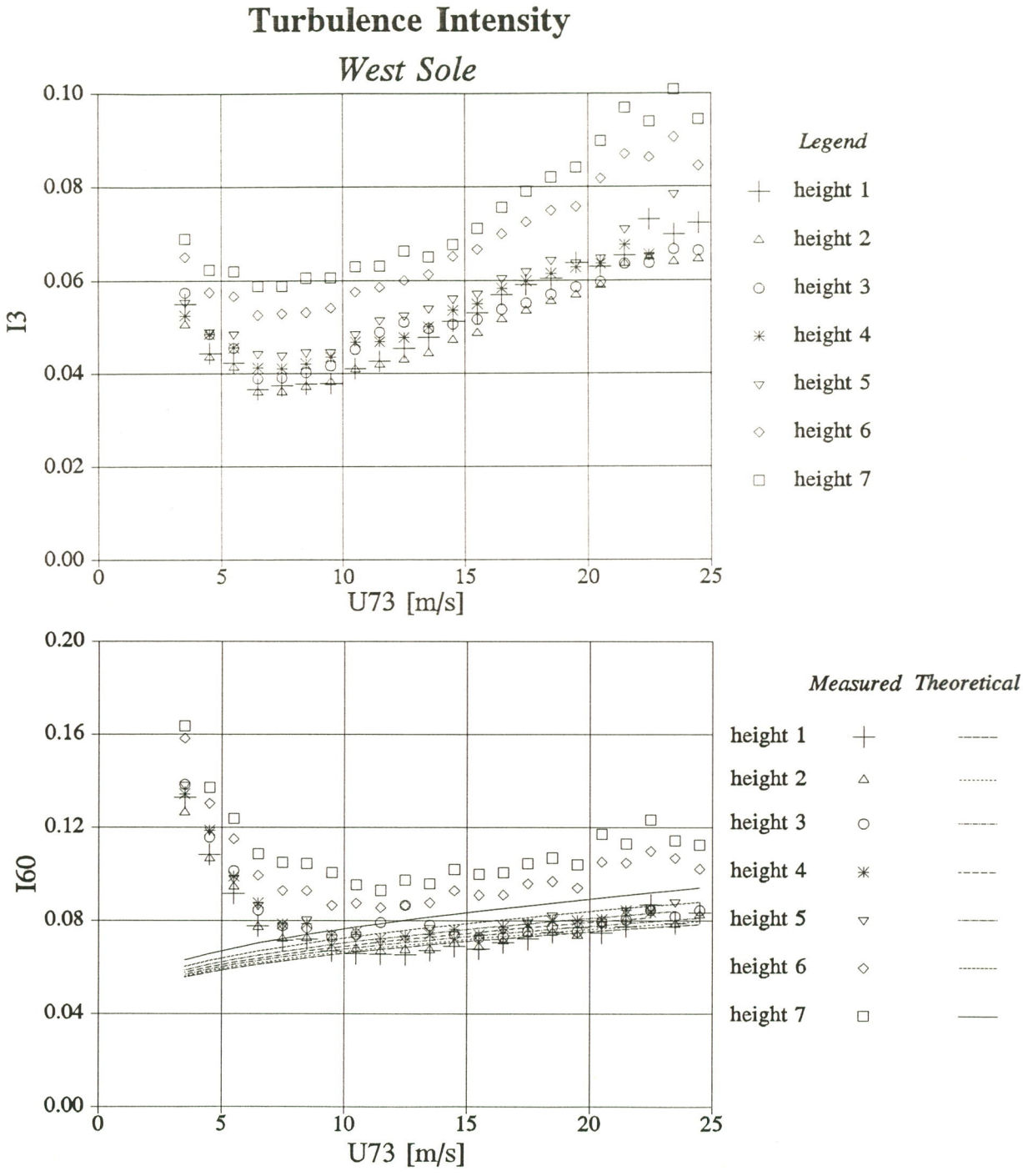

Figure 4.10a-b The turbulence intensities versus wind speed at the measuring heights
a) I_3
b) I_{60}

4.6.2 Influence of stability on turbulence intensity

The stability of the atmosphere can be characterized by means of the Obukhov length L. The Obukhov length is described in detail in chapter 2. Essentially, it is a measure for the ratio between mechanical turbulent energy transport and convective transport. The Obukhov length has been determined using the procedure described by Van Wijk et al. [1990].

As was noted in section 4.4.6 the temperature difference T_{air}-T_{sea} is essential for the procedure. The use of the long term database makes it by all means possible that the sea water temperature differs from the real temperature at the West Sole platform. This seriously limits the significance of the present analysis. Nevertheless we will show that the analysis made in this way offers some insight in the behaviour of the turbulent intensity with stability.

Figures 4.11 shows the turbulence intensity I_3 as a function of the wind speed discriminated by the stability at measuring level 2. The graph shows the difference between a stable, unstable and neutral atmosphere. In the stable atmosphere turbulence is suppressed and lower than in a neutral atmosphere. The neutral case closely follows the theoretical curve. The unstable situations are marked by their higher turbulence intensity level.

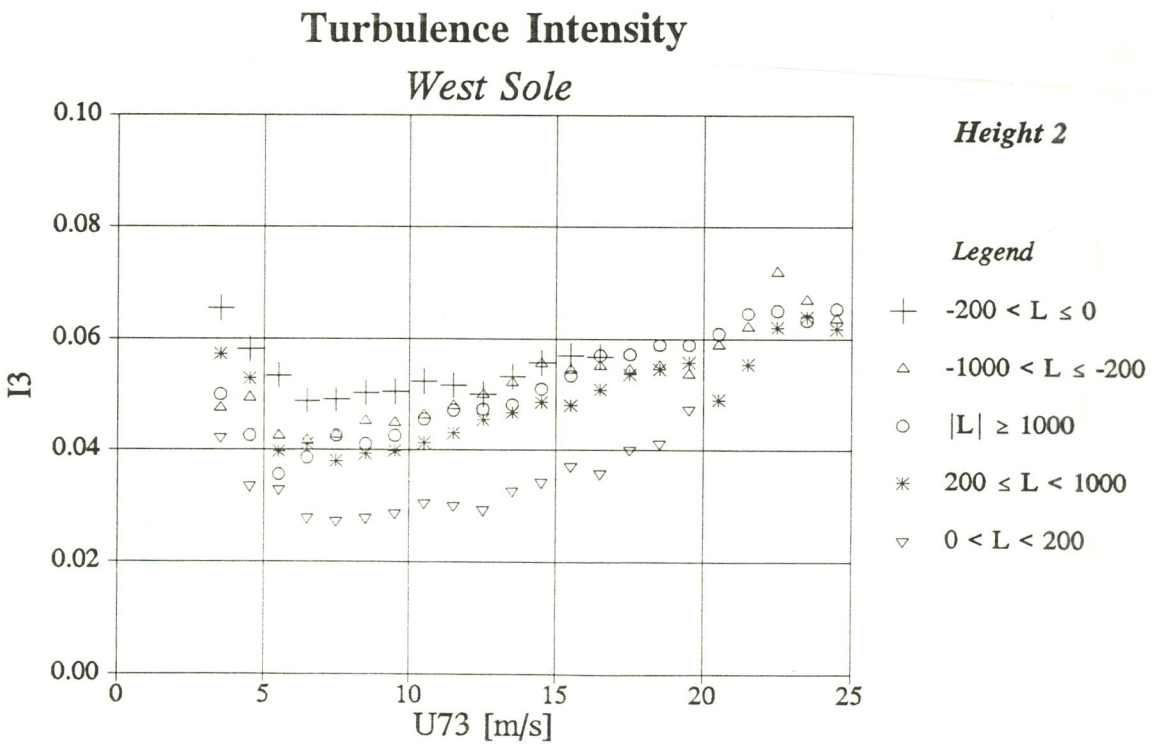

Figure 4.11The turbulence intensity I_3 as a function of wind speed and stability class for level 2.

5 Comparison of K13 and Light Vessel Texel

5.1 Introduction

Until the 80s, the knowledge of the wind climate of the North Sea originated from data of light vessels and voluntary observing ships. Over the years these databases have been studied extensively [Korevaar, 1987; Korevaar, 1989]. Although these databases are consistent over very long periods of time (sometimes more than 100 years), these wind speed data consist of Beaufort estimates instead of anemometer measurements, so they cannot be compared in all respects with the measurements at West Sole or K13.

In this section some of the analyses of Light Vessel Texel will be compared with the results of K13. Although the periods are different, this comparison may give an indication of the quality and the consistency of the K13 database.

5.2 Results

5.2.1 Overall mean wind speed and interannual variations

During the 11-year period of 1966-1976 the overall mean wind speed at 10 meters height at LV Texel was 7.3 m/s, according to Wieringa and Rijkoort [1983]. For the period 1971-1976 a more detailed analysis could be made of LV Texel, because these data were available to us. The overall mean wind speed during this period was 7.4 m/s. In table 5.1 the interannual variations are shown for this period. Using the diabatic wind profile the mean wind speed at 10 m height at K13 in the period 1982-1989 is calculated also. This results in a value of 7.7 m/s, which compares quite well with the mean wind speed at LV Texel, both during 1971-1976 and 1966-1976.

For the period 1971-1976 the interannual variations of the wind speed at LV Texel is shown in table 5.1.

Table 5.1 Annual mean wind speeds at LV Texel (1971-1976)

year	annual mean wind speed [m/s]
1971	7.02
1972	7.35
1973	7.32
1974	7.96
1975	7.37
1976	7.22
1971-1976	7.37

From the table it can be seen that the interannual variations are between -5% and +8%. This seems to be much less than at K13, but it must be kept in mind that, compared to the K13 database, this time period is shorter, and not the same.

5.2.2 Frequency distribution and Weibull parameters

The analysis of the frequency distribution of LV Texel results in a Weibull k factor of 2.14 for the period 1966-1976, as reported by Wieringa and Rijkoort [1983], while the analysis of the period 1971-1976 resulted in a Weibull k factor of 2.07. Again using the logarithmic wind profile to calculate the wind speed at 10 m height at K13, a value of 2.07 for k is found.

5.2.3 Annual course

The annual courses of the wind speeds are compared. For LV Texel data are used of the periods 1971-1976 and 1966-1976 [Wieringa and Rijkoort, 1983], for K13 of the period 1982-1988.

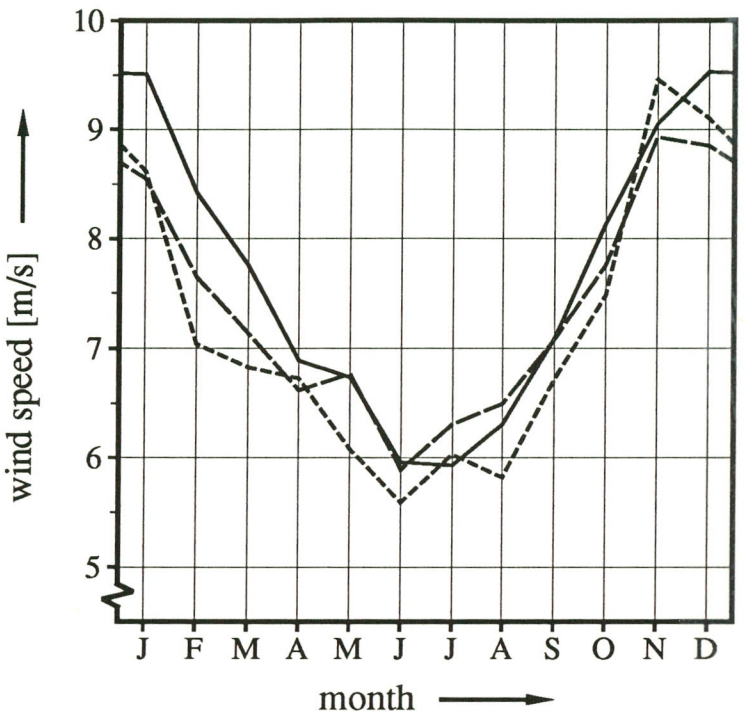

Figure 5.1 Annual courses of the wind speeds at 10 m at K13 (1982-1988; solid line) and LV Texel (1971-1976; short dashes, and 1966-1976; long dashes [Wieringa and Rijkoort, 1983]).

It can be seen from figure 5.1 that the annual courses of K13 and LV Texel are quite similar. The difference is that the maximum wind speed at LV Texel occurs in November, while at K13 this occurs in December-January.

5.2.4 Diurnal course

The diurnal courses have also been compared. In figure 5.2 the diurnal courses are shown, for K13 of the period 1982-1988, for LV Texel for the periods 1971-1976 and 1966-1976 [Wieringa and Rijkoort, 1983].

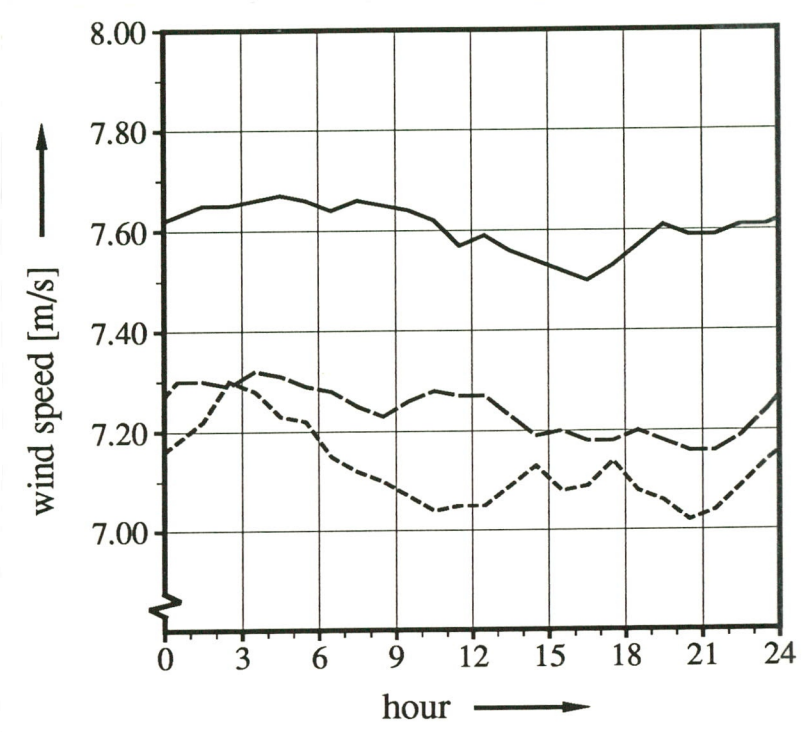

Figure 5.2 Diurnal courses of the wind speeds at 10 m at K13 (1982-1988; solid line) and LV Texel (1971-1976; short dashes, and 1966-1976; long dashes [Wieringa and Rijkoort, 1983]).

Figure 5.2 shows similar diurnal courses for K13 and LV Texel. There seems to be a slight tendency for wind speeds to be higher during night hours than during day hours.

5.2.5 Statistics by windsector

The results by windsector of K13 and LV Texel have been compared. Table 5.2 shows the mean wind speeds at 10 m height for LV Texel (1971-1976) and for K13 (1982-1988). Also shown are the frequencies of occurrence of each windsector for LV Texel and K13 during the same periods.

Table 5.2 Mean wind speeds at 10 m and frequencies of occurrence by windsector at K13 (1982-1988) and LV Texel (1971-1976)

wind sector	frequency of occcurrence %		wind speed [m/s]	
	K13	LV Texel	K13	LV Texel
1	5.9	7.4	6.2	6.8
2	6.4	8.2	6.2	6.3
3	5.6	6.8	7.0	6.6
4	6.7	8.6	7.5	6.5
5	5.2	5.9	6.4	6.2
6	5.6	4.7	6.7	6.3
7	8.2	8.6	7.5	7.3
8	14.0	12.4	8.7	8.0
9	13.7	10.9	8.4	8.1
10	11.8	11.1	8.5	8.2
11	8.6	8.7	7.3	8.2
12	7.7	6.7	6.7	7.8

It can be concluded that the figures for K13 and LV Texel are quite similar.

5.2.6 Air and seawater temperatures

Stability conditions are determined by the temperature difference of air and seawater (surface). For comparison between LV Texel and K13, it is interesting to study the annual courses of the temperatures of air and seawater, and of the temperature difference. In figures 5.3a-d these annual courses are shown.

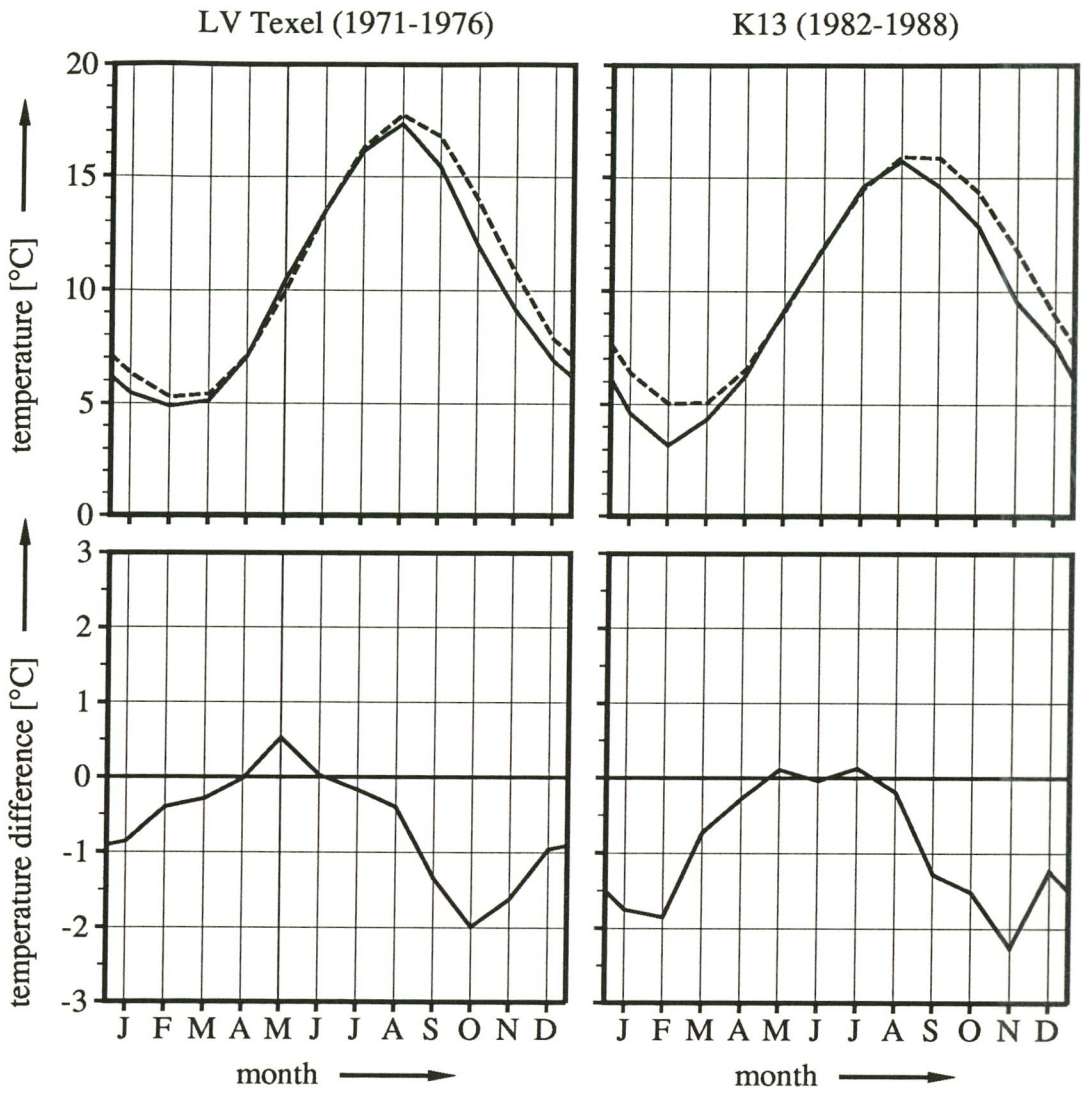

Figure 5.3a-d Annual courses of air (solid lines) and seawater (dashed lines) temperatures and temperature differences at K13 (1982-1988) and LV Texel (1971-1976).

The figures show that these annual courses are quite similar at LV Texel and at K13. The period of K13 contains some extremely cold years, which probably accounts (partly) for the fact that the temperatures are somewhat lower at K13 than at LV Texel. This similarity implies a similarity in stability conditions over the year also.

5.2.7 Statistics of stability

In the table 5.3 the statistics of stability for K13 (1982-1988) and LV Texel (1971-1976) have been compared, based on the values of L.

Table 5.3 Comparison of statistics of stability at K13 (1982-1988) and LV Texel (1971-1976)

stability conditions	value of L	frequency of occurrence %	
		K13	LV Texel
Very stable	0m<L<200m	10.3	19.8
Stable	200m≤L<1000m	13.3	14.0
Neutral	|L|≥1000m	12.1	14.9
Unstable	-1000m<L≤-200m	12.2	14.1
Very unstable	-200m<L≤0m	48.1	36.2

From this table it can be seen that at LV Texel (very) unstable conditions prevail (50.3% of the time), although the very stable class also has a high frequency of occurrence.

5.2.8 Geostrophic wind

The calculation of the geostrophic wind speeds is described in section 2.3.1. For comparison this has also been done for LV Texel. The results for the years 1971-1976 are shown in table 5.4.

Table 5.4 Mean geostrophic wind speeds and Weibull parameters at LV Texel (1971-1976) and K13 (1982-1988)

Expression used	LV Texel				K13			
	wind speed [m/s]	k	a [m/s]	U_{mean} [m/s]	wind speed [m/s]	k	a [m/s]	U_{mean} [m/s]
(2.4)	10.12	2.26	10.78	9.55	10.16	1.75	11.21	9.98
(2.7)	10.30	2.18	10.97	9.72	10.53	1.78	11.56	10.29
(2.8)	10.16	2.24	10.84	9.61	10.38	1.78	11.46	10.20
(2.11)	10.5	-	-	-	10.5	-	-	-

For the results at LV Texel the same can be concluded as at K13: the neutrally calculated mean geostrophic wind speed is higher than the diabatically calculated values. The values found at LV Texel are also in quite good agreement with the values found at K13. The values of the Weibull k parameter are highly different from the K13 values. It must be kept in mind, however, that the periods are different and that LV Texel is located much nearer to the main land.
The value for the mean geostrophic wind speed found by using (2.11) is somewhat higher compared to the other values. Due to the coarseness of the grid the values at K13 and LV Texel are the same.

Lundtang Petersen et al. [1981] have analysed pressure data to derive the geostrophic wind field over Denmark. Using data from 7 meteorological stations throughout Denmark over the period 1965-1977, mean geostrophic wind speeds ranging from 10.1 m/s to 11.3 m/s were found. It was assumed that the geostrophic wind varies so little over Denmark, that no geographical variations have to be incorporated. The geostrophic wind field is described sufficiently by wind speeds and wind speed distributions by wind direction. The overall mean geostrophic wind speed resulted in a value of 10.2 m/s, with a Weibull k parameter of 1.75 and a Weibull a parameter of 11.48 m/s. These values are in good agreement with the results of K13.

Although at LV Texel wind speeds were never measured with an anemometer but were derived visually from wave characteristics using the Beaufort scale, the comparison of these data for a limited period of 11 or 6 years (depending on the availability of the data), with the data measured at K13 during only 8 years, on a platform that is still in use as a gas production platform, gives satisfactory results. The availability of measured data at K13 is very high, and no inconsistencies have been encountered, having looked at annual courses, diurnal courses, Weibull distributions, wind speeds by wind direction etc. Comparison of geostrophic wind speeds calculated with three different methods also results in similar results for the mean values, but not so much for the Weibull k parameters. These mean geostrophic wind speeds are much lower (2-3 m/s) than those suggested by Wieringa and Rijkoort [1983].

Therefore, the conclusion seems justified, that the results of K13 and LV Texel both give an adequate description of the North Sea climate on a local scale.

6 Wind turbine design loads

6.1 Introduction

In order to design safe and reliable machines designers need accurate wind input data for their load calculations. In the Netherlands these design wind load data are provided by the Handbook Wind Data for Wind Turbine Design, version 3 [Verheij et al., 1991], which is an important document in the certification procedure. This Handbook offers design data in the form of discrete gusts with prescribed time duration and amplitude. At present these data are not available for offshore conditions.

In the near future, load calculations will probably be carried out more often using time sequential wind speed data computed with a Stochastic Wind Simulator. The input for such a simulator consists of power spectra and coherence functions of the turbulent wind.

In this chapter we give a review of the spectral characteristics of offshore turbulent wind, obtained from a literature survey. Further, we discuss the differences between an 'offshore' and the 'onshore' Handbook and draw conclusions regarding missing information.

6.2 Spectral characteristics of turbulent wind

In the literature only scarce information can be found on spectral characteristics of offshore wind. The information which is available comes mainly from measurements at offshore structure supplied with meteorological equipment [Wills, 1990; Eidsvik, 1985]. Wills and Eidsvik have been taking fast-rated measurements which enabled them to determine turbulence spectra of the u-component and in case of Wills also correlation and coherence functions.

Another type of experiments was made by Nicholls and Reading [1980], who took measurements during a number of research flights with a Hercules C30 airplane over the North Sea. Using the data of these flights, spectra of the various wind components, estimates for the Reynolds stresses, heat and humidity fluxes were derived.

6.2.1 Spectra

In wind energy applications and for engineering purposes often the Kaimal spectrum is used to describe the power spectrum of the turbulent energy [Panofsky and Dutton, 1985; Kaimal, 1972]. The Kaimal spectrum is an empirical relation, derived for neutral weather conditions, based on field experiments. It writes.

$$\frac{nS_U(n)}{\sigma^2} = \frac{n/n_m}{(1+1.5n/n_m)^{5/3}} \qquad (6.1)$$

n denotes the non-dimensional frequency n = fz/U, in which f is the frequency, z the measuring height and U the mean wind speed. The power spectrum is normalized by the standard deviation of the wind speed fluctuations σ_U, so that the integration over all frequencies yields unity. n_m is the normalized frequency, for which the spectrum shows a maximum. The value of n_m has been empirically determined and is equal to 0.046. Sometimes the spectrum is not normalized by σ_U, but by the friction velocity u_*, in which case the nominator becomes $4.8\ n/n_m$. In the high frequency range (6.1) becomes proportional to $(n/n_m)^{-2/3}$. Here the turbulence is in the inertial sub-range.

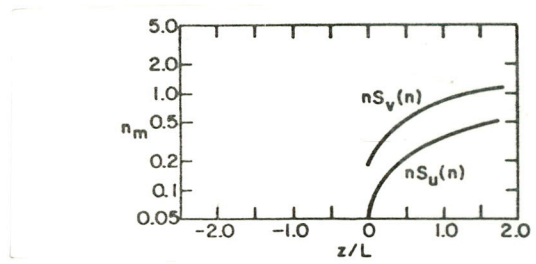

Figure 6.1 Normalized peak frequency n_m for u and v spectra in stable air [Kaimal, 1972]

In stable air, Panofsky and Dutton argue that (6.1) still holds except that n_m has to be adjusted. Figure 6.1 gives a relation for n_m as a function of the stability parameter z/L.

In unstable weather conditions the energy content at low frequencies is much higher than in neutral conditions. The spectrum has to be adjusted accordingly. Experiments seem to indicate that the peak of the power spectrum does not scale with the height z, but is rather constant. It is found that at lower frequencies the power spectrum does not scale with the height z, but scales with the inversion layer height z_i. Højstrup [1982] has derived an empirical formula which describes this behaviour

$$\frac{nS_U(n)}{u_*^2} = \frac{0.5n_i}{1+2.2n_i^{5/3}}\left(\frac{z_i}{-L}\right)^{2/3} + \frac{105n}{(1+1.5n)^{5/3}} \qquad (6.2)$$

where n_i denotes the non-dimensional frequency fz_i/U. Figure 6.2 shows this relation for several values of the parameter n_i. The inversion layer height is related to the mixing height and can be determined from amongst others the friction velocity. It seems that the Højstrup spectrum follows the Kaimal spectrum rather closely when z and z_i are of the same order.

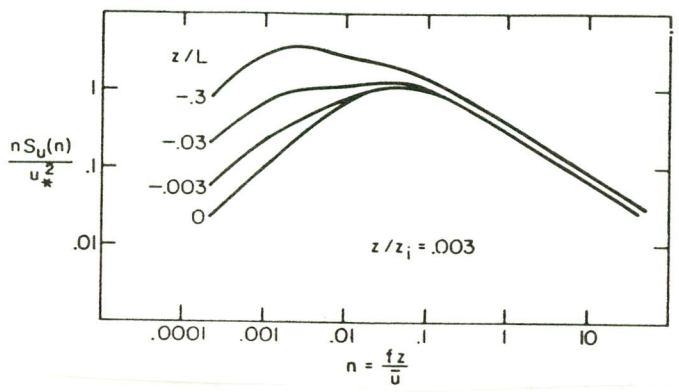

Figure 6.2 u spectra in unstable air for fixed z/z_i, after [Højstrup, 1981].

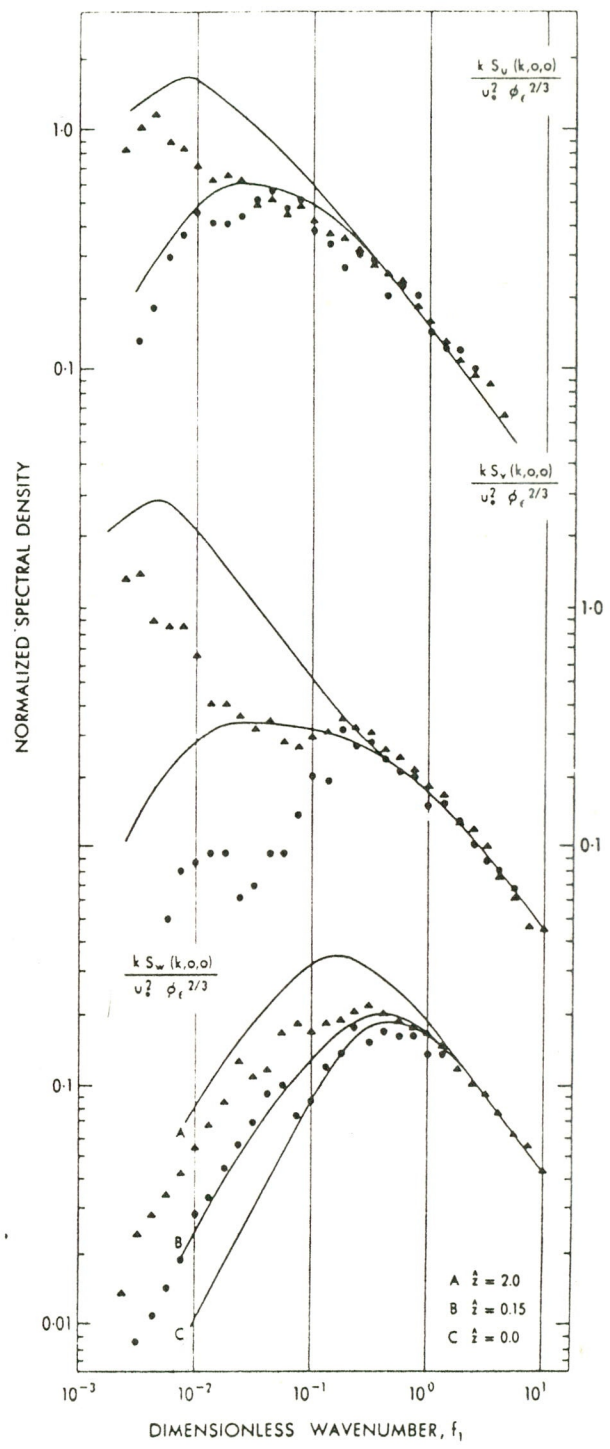

Figure 6.3 Normalized along-wind sampled velocity spectra (class means plotted) [Nicholls and Readings, 1980]
▲ - class I (more unstable, z/L > 0.15),
• - class II (less unstable, z/L < 0.15). The curves represent results obtained over land by Kaimal et al.

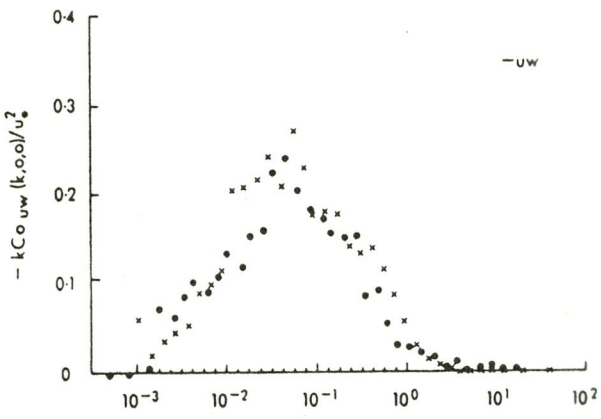

Figure 6.4 Normalized along-wind co-spectrum -uw, classes I and II combined, denoted •. X Results from other experiments [Nicholls and Readings, 1980].

Nicholls and Readings [1980] performed measurements during a number of research flights at several measuring heights ranging from 30 m to 230 m. Fluctuations on the average wind velocities were obtained by removal of the mean and linear trend calculated along each flight leg (about 60 km in most cases). In addition high frequency noise was removed from the velocity components. The stability covered by the dataset ranged from $0 < z_i \leq 10$, where z_i denotes the height of the first inversion layer and L is the Monin-Obukhov length. For the analyses data were selected for the lowest flight levels only, such that they only applied to the surface layer, where the authors expected that the Kaimal spectrum could be applied and the influence of the inversion layer height could be neglected. Figure 6.3 gives the main results of the analysis. The abscissa is given by the non-dimensional frequency n = fz/U, where f denotes the frequency, z the measuring height and U the average wind speed. The spectrum was brought into non-dimensional form by dividing fS(F) by $u_*\phi_\varepsilon^{2/3}$, In which ϕ_ε is a function given by the dissipation of the smaller eddies. The two sets of data in the figure show measuring situations with different levels of stability. The high curve is the situation where -z/L>0.15 (more unstable) and -z/L<0.15 (less unstable).
Figure 6.4 shows the co-spectrum for the uv-component of the turbulent shear stress averaged over the two stability classes.
The authors conclude that the spectra and co-spectra of the velocity components agree well with previous measurements over sea in similar conditions and that they are also very similar to the measurements made by Kaimal over land. The measurements further show that in the low frequency region there is significant discrepancy among the various stability classes.

In the period from June 1979 to April 1982 wind speed measurements (among other measurements) were taken at the top of the Statfjord drilling derrick, located at 61.5•N, 2.5•E. These measurements have been described by Eidsvik [1985]. A total of 3662 20-minute time series were recorded. The standard sampling program consisted of T = 20 min time series every 3 hours. The sampling rate was approximately 1 second. Due to the wind disturbance by the structure the wind

recordings are probably contaminated by wake effects. For some of the time series there exist simultaneous data for wind direction and air-sea temperature difference. However the sea temperature was not used as a parameter in the study.

The high frequency spectrum was fitted to the Kolmogorov's inertial sub-range law in order to find the parameters α_k and ε (ε is the turbulent dissipation) in the expression

$$kS(k) = \alpha_k \varepsilon^{2/3} k^{2/3} \tag{6.3}$$

which was also used in the paper of Nicholls and Readings. Here, k denotes the wave number of the turbulence, and can be transformed to a frequency by using Taylor's hypothesis. The fit was used to determine the parameter n_m in the Kaimal frequency spectrum, which in the high frequency limit approaches Kolmogorov's law.
The experiments give some evidence that the peak in the spectrum is not at a fixed normalized frequency n, but rather at a fixed frequency f (see figure 6.5) in contrast with other estimates.
Eidsvik shows that the low frequency content of the spectrum is much higher than it is in the Kaimal spectrum. The fact that other studies don't show this behaviour the author explains by the commonly used trend removal techniques.
Although Eidsvik did not find simple linear relationships between the low frequency content and standard weather conditions, he does seem to find a relation with the air-sea temperature difference. As we have seen the stability of the boundary layer is highly dependent on this temperature difference.

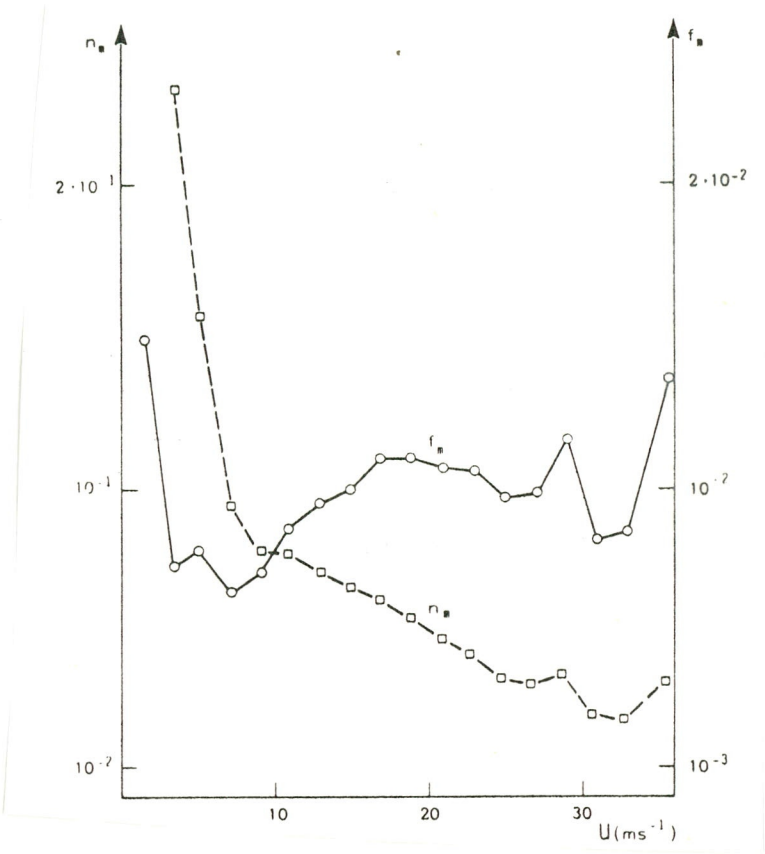

Figure 6.5 Average 'maximum' f_m and n_m in Kaimal's model spectrum for different mean wind classes [Eidsvik, 1985].

At West Sole spectra were calculated from the fast-sampling experiments carried out mainly at high winds [Wills, 1990]. As described in chapter 3, the seven anemometers on the windward side were sampled simultaneously at a rate of five per second for 128 minutes and recorded. The results were binned with respect to wind speed. Figure 6.6 (32) shows the spectra S(f) versus frequency f for the wind speed band 20-25 m/s. Only the 4 topmost levels have been plotted. The spectra have been plotted on a double logarithmic scale, which clearly shows the inertial sub-range law at the higher frequencies.
Wills has compared the spectra with Kaimal's empirical relation as listed above and concludes that the spectra follows this relation for the higher frequencies, but that it shows a somewhat lower peak value, when fS(f) is plotted against f. The measurements show a higher energy content at lower frequencies than predicted by the Kaimal spectrum. This is in agreement with the measurements analysed by Eidsvik. Wills uses a modified Kaimal-spectrum to describe the experimental results.

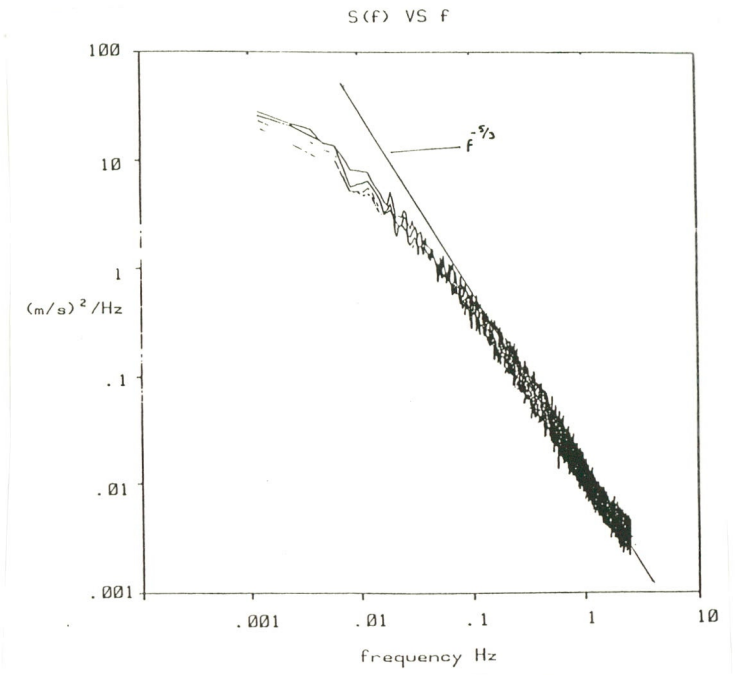

Figure 6.6 Turbulence spectra, 20-25 m/s [Wills, 1990].

6.2.2 Coherence

The coherence function is generally taken as

$$Coh_{\Delta z}(f) = exp(-a_z.f\Delta z/V) \tag{6.4}$$

The quantity a_z is the decay constant for vertical separations, a_z depends on the height z and on the stability of the boundary layer. According to Panofsky and Dutton the decay constant is given by

$$a_z = 12 + 11\Delta z/z$$

for neutral atmospheres.

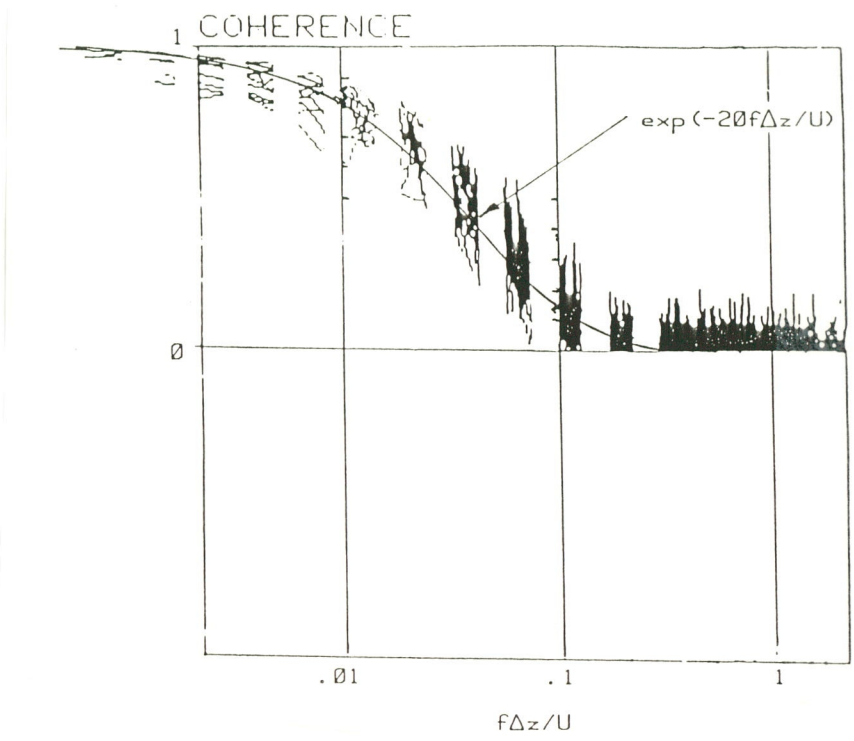

Figure 6.7 Measured coherence function [Wills, 1990].

The measurements at West Sole are the only experiments known to us for which coherence functions over sea have been determined. The coherence among the various measuring heights was determined and compared to literature values.
The analysis indicates that the measured coherence function follows the exponential shape (see figure 6.7). The decay constant a_z found in the experiments is 20 rather higher than Davenport's value over land of 16. The more rapid decay at high frequencies is consistent with the results quoted above from Panofsky and Dutton.

6.3 Handbook Wind Data for Wind Turbine Design

The Handbook Wind Data for Wind Turbine Design [Verheij et al., 1991] has been developed to supply wind data for load calculations in onshore situations. In the future wind turbines will be designed for offshore applications, and it is likely that the Handbook should be supplemented to deal with this different environment. Below we will make an inventory of the expected differences, and where applicable make recommendations for adaptations.

Wind speed distribution
The Handbook recommends to use the Den Helder wind speed distribution for load calculations. Since the wind speeds offshore are higher than onshore the wind speed distribution should be adapted for offshore applications. At present only the K13 wind speed frequency distribution is available. In table 6.1 the Weibull parameters of Den Helder and K13 are compared.

Table 6.1 The Weibull parameters of the wind speed distribution at 10 m height at Den Helder and K13

	k_{10}	U_{10}
LV Texel	2.14	7.37 m/s
Den Helder	2.00	6.67 m/s
K13	2.06	7.69 m/s

Two remarks should be made in this context:
1. Until now, the spatial distribution of the wind resources over the North Sea is unknown. However, large differences are not expected and hence it is advised to use the K13 Weibull parameters;
2. The Den Helder data represent the potential wind speed (10 m height, z0 = 0.03 m). The data for K13 represent the wind speed scaled to 10 m using Monin-Obukhov similarity theory (see Chapter 4). Hence, the results should be handled with care.

Turbulence intensity
Typically, mechanical turbulence offshore is low compared to onshore situations. Using the Example data from the Handbook (Chapter 9) the turbulence intensity at hub height (30 m) is I = 0.18.
The turbulence intensity measured at West Sole interpolated to 30 m level and taken at the average wind speed is I_{60} = 0.08.

In chapter 2 we have shown that for the u-component of the turbulence intensity the same expression can be applied as used in the handbook, taking care that the correct roughness length is applied. In contrast with the onshore situation the roughness length z_0 is dependent on the wind speed, according to the Charnock relation. However, figure 3.11 shows above a wind speed of 10 m/s the variation with wind speed is rather small, and that it is probably sufficient to select one typical value for z_0.

The turbulence intensity depends on the stability of the atmosphere. In a stable atmosphere turbulence is suppressed by the thermal stratification, in an unstable atmosphere thermal convection enhances turbulence. In the Handbook stability is neglected altogether by arguing that for high wind speeds mechanical turbulence always dominates the thermally driven turbulence. The analysis has shown that different turbulence intensity levels occur for different stability classes. The present dataset is not sufficiently accurate to draw firm conclusions, taking into consideration the uncertainty in the sea surface temperature. In order to draw conclusions on the importance of stability on the turbulence intensity, the probability of occurrence of the various stability classes should be determined as a function of the average wind speed.

No information was found on the lateral turbulence intensities, which is important for the derivation of wind direction fluctuations. However, it is assumed that the rate between longitudinal and lateral turbulence intensities is about equal for both offshore and land locations.

Fatigue gusts
The expressions which are used in the handbook were derived from time histories of turbulent wind measured at the meteorological mast of Cabauw. The amplitude of a fatigue gust have been given as a function of several parameters:
— the hub height,
— the turbulence intensity,
— the gust duration,
— the average wind speed.

Similar measurements are not available from offshore measuring masts. It is highly unlikely that the same expressions hold under offshore conditions.
Therefore, either similar expressions should be derived by applying gust analysis to wind speed time series measured at an offshore measuring mast.
An alternative approach might be to obtain accurate expressions of turbulent power density spectra and coherence functions, which could be used as input in a stochastic wind simulator. A disadvantage of this approach is the lack of information about gusts occurring only a couple of times per hour and less (probability of occurrence of about 1% and less).

Wind shear
The smooth water surface an its small roughness length causes a lower wind shear than is found over land. For instance, the example calculation in the handbook with hub height H = 30 m, rotor diameter D = 25 m yields a wind shear over 3/4 rotor diameter of $A_g = 0.068$ U (table 6.2). Assuming the same data in the offshore situation, with a roughness length $z_0 = 0.0002$ m, the wind shear becomes $A_g = 0.027$ U.

In principle the wind shear depends on the average wind speed through the Charnock relation. However, the wind shear is rather insensitive to the small changes in roughness, so probably one single (conservatively chosen) value could be applied for load calculations. For instance, taken an average wind speed of 25 m/s, the wind shear becomes $A_g = 0.032$ U.

Table 6.2 Overview of wind shear for an example wind turbine, H = 30m, D = 25 m

condition	wind speed	z_0	L	A_g
land	-	0.25m	∞	0.068U
offshore	8.5 m/s	0.0002m	∞	0.027U
offshore	25.0 m/s	0.0012m	∞	0.032U
offshore	8.5 m/s	0.0002m	200m	0.041U
offshore	8.5 m/s	0.0002m	-200m	0.019U

Stability can have a more significant effect on wind shear. In stable weather the wind shear can increase considerably, e.g. with the Obukhov length L = 200 the wind shear becomes $A_g = 0.041$ U in our example calculation. In unstable weather the wind shear decreases due to the enhanced mixing: with L = -200 the wind shear $A_g = 0.019$ U.
The wind shear as a function of stability is shown in figure 6.8 for this particular example.

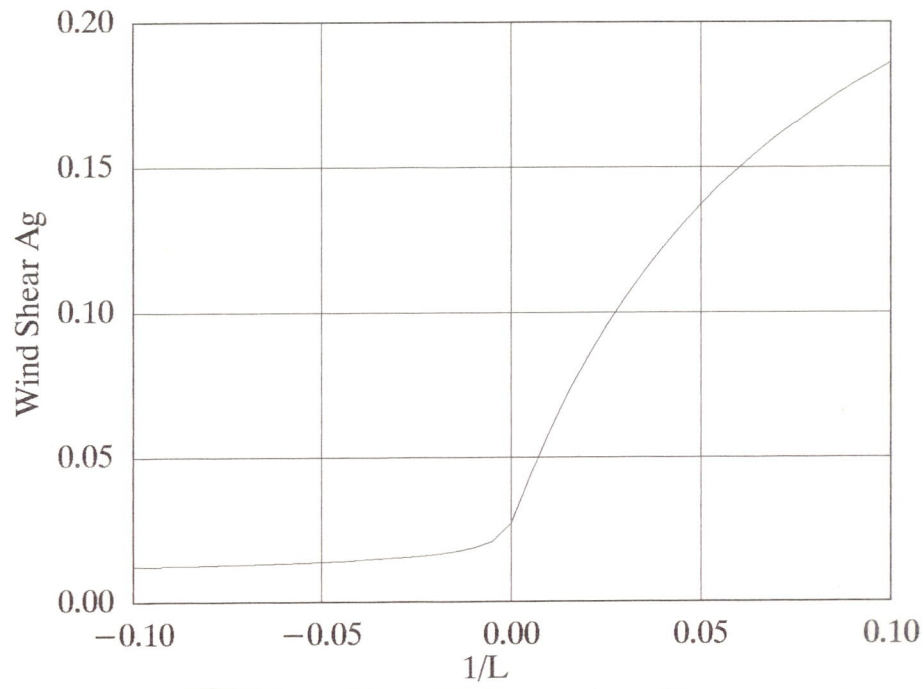

Figure 6.8 Wind shear as a function of 1/L using the diabatic wind profile with z_0 = 0.0002 m according to (2.3), for a wind turbine with a hub height of 30 m and a rotor diameter of 25 m.

It is important to note that sea stability varies seasonally (caused by the air-sea temperature difference), in contrast over land where it has mainly a diurnal character.

Rotational sampling
The formalism used to derive the expressions for rotor averaging and rotational sampling does not change in an offshore situation. The expressions derived for the various amplitudes do however depend on the coherence function in the rotor plane. Very few experimental coherence function are known, which were measured offshore. The measurements of Wills seem to indicate that the coherence function does not differ too much from that over land (see section 6.2.2). Probably, the expressions used in the Handbook, therefore don't need to be changed.

Voorgedaan

Extreme wind conditions

In the present study no attempt was made to describe extreme wind conditions. In the Handbook extreme wind conditions are divided into extreme gusts and extreme wind speeds. The former are based on a Fisher-Tippet-I frequency distribution of wind speed fluctuations. This might also be applied for the offshore locations. The latter is based on an extreme hourly mean wind speed on which a gust amplitude is added. The gust amplitude is dependent on the turbulence intensity. Since wind speeds are generally higher offshore and turbulence intensities lower it is not exactly known what the final effect is on the extreme wind speeds.

Wind farms

The section on turbine loads in wind farms is in the Handbook rather brief. It is expected that this section will be extended in the future. Offshore wind farms are different in some aspects from onshore wind farms:

1. In offshore wind farms the turbulence level is probably lower than in land based wind farms, hence causing smaller loads,
2. On the other hand, since the ambient turbulence is lower, the recovery of wakes is less rapid in an offshore wind farm. This brings about higher horizontal shear in the wind farm, which can increase the loading on the wind turbine.

The results of the JOULE-projects Wake and Wind Farm Modelling, Dynamic Loads in Wind Farms and Full-Scale Measurements in Wind Turbine Arrays will provide additional data on this subject.

7 Conclusions and recommendations

7.1 Introduction

This chapter summarizes the main conclusions of the report. Further, the results of the analysis of the wind climate are reviewed.
In section 7.3 the areas of insufficient data or knowledge in the field of wind data for wind energy estimates are identified and areas of future research are identified. In section 7.4 the same has been done for the field wind data for wind turbine design.

7.2 Conclusions

7.2.1 Wind Climate

Wind speed measurements from the K13 platform in the North Sea are suitable for studying the wind climate of the North Sea. The reliability during the period 1982-1989 is very high (the availability of 10-minute wind speed values is 97%). The mean wind speed at a height of 74.9 meters above MSL during this period was 9.00 m/s. Table 7.1 gives the mean wind speed and the Weibull parameters of the wind climate at K13 in the period 1982-1988.

The West Sole data are not suited for studying the wind climate, because of the short measuring period. Comparison of the monthly mean wind speeds of K13 and West Sole, simultaneously measured at approximately 75 m height shows that these are between 1 m/s and 3.5 m/s lower at K13 than at West Sole.

Table 7.1 Wind climate at K13 and LV Texel

Station	height	U_{mean}	k
K13	74.9 m	9.00 m/s	2.04
K13	10 m	7.7 m/s	2.07
LV Texel	10 m	7.3 m/s	2.23

Table 7.1 also shows the results of the comparison between the K13 wind speed measurements and the Beaufort wind speed estimates of LV Texel in the period 1966-1976. The calculated mean wind speed at K13 for a height of 10 m compares quite well with the value at LV Texel. This leads us to the conclusion that, based on the results of K13, the use of LV Texel in the Dutch Handbook for Wind Energy Production Estimates for climatological purposes, seems justified.

At K13 the interannual variations of the average of 10-minute wind speeds are between +14% and -16%, which seems to be larger than on land.

Offshore, there is a larger seasonal variation in the wind speed than over land. The monthly mean wind speeds deviate from the annual mean wind speed between +26% and -22%. An maximum monthly mean of 11.8 m/s occurs in January and a minimum of 7.0 m/s is found in June.

No significant diurnal course was found at K13. The observed diurnal variations on the mean wind speed are less than ±1%.

The distribution of wind directions of K13 shows that the prevailing wind direction is southwesterly (sector 7 to 10), the wind direction is within these sectors nearly half of the time. The mean wind speed is the highest in these sectors as well (9.09-10.06 m/s).

7.2.2 Stability

The stability conditions of the boundary layer depend in general on the temperature difference of air and seawater, as well as on the wind speed. The air temperature was measured simultaneously with the wind speed measurements. The seawater temperature was obtained from data recorded by Voluntary Observing Ships in case of the K13 platform and from a Historical Dataset in case of the West Sole platform.

The annual courses of the air and seawater temperature show that the temperatures vary sinusoidally, with the higher temperatures during the summer and low temperatures in wintertime. The K13 data show that during the winter the air temperature is lower than the seawater temperature, while in the summer the situation is the other way around. On the average the air temperature was 0.9 °C lower than the seawater temperature.
In case of West Sole the air temperature is higher than the seawater temperature throughout the year. This is brought about by the use of the historical dataset, which was not measured simultaneously with the air temperatures, and does not represent the real physical situation.
In order to determine the correct temperature difference it is hence necessary to have available simultaneously measured seawater and air temperatures.

The statistics of stability conditions show that unstable conditions prevail at K13. At West Sole, on the other hand, stable conditions seem to prevail, but we believe that this result is brought about by the erroneous temperature data and does not reflect the real situation.

7.2.3 Wind Profile

Wind speeds at K13 calculated for a height of 10 m above MSL with the diabatic and the logarithmic wind profile, result in almost the same value: 7.66 m/s and 7.57 m/s, respectively. The influence of stability does not seem to affect the annual mean wind speed.

The overall mean calculated roughness length is 0.00017 m, which matches the generally accepted mean value of 0.0002 m. The extreme values, however, range from 0.00002 m to 0.00055 m, depending strongly on the wind speed.

Wind profiles calculated with the diabatic model have been compared with the wind speeds in the West Sole dataset. The uncertainties in the temperature dataset prevent solid conclusions on the validity of the diabatic model.

7.2.4 Geostrophic wind

The PBL height depends on stability conditions. For neutral conditions the mean PBL height is 1123 m, while for very stable conditions the mean PBL height is only 107 m. In very stable conditions situations may occur that the height of the PBL is less than the measuring height of the wind speed (74.9 m above MSL). In such situations the measured wind speed can in fact be interpreted as the geostrophic wind speed.

The value for the mean geostrophic wind speeds at K13, calculated using four different methods, ranged from 10.2 m/s to 10.5 m/s. For LV Texel nearly the same values were found. Moreover, these values are in the same range as results given by the European and Danish wind atlases. Compared with these results, the results given by Wieringa and Rijkoort [1983] based on land based stations seem to high (13 m/s).
It can be concluded that the mean geostrophic wind field calculated using pressure data or surface wind speed data compare well. More detailed information such as frequency distributions and annual courses, however, can only be derived using surface wind speed data.

7.2.5 Turbulence

The measurements at West Sole show that the turbulence intensity offshore is considerably lower than over land. Above a wind speed of approximately 10 m/s mechanical turbulence dominates over convective turbulence. In that range the turbulence intensity is described well by a simple expression when using the correct roughness length according to the Charnock relation. Typically, a turbulence intensity of 8-10% is found at all heights. The lowest levels show higher turbulence levels, but these levels are disturbed by the West Sole main deck.
For lower wind speeds the average turbulence intensity is higher, which can be explained by the influence of stability.

Information on the spectral characteristics of offshore wind is scarce. The information which is available comes from low level research flights with airplanes and from fast rate measurements taken at a few instrumented offshore platforms. The experiments indicate that the power spectra of the turbulent wind follow the well-known Kaimal-spectrum for the higher frequencies, but that at lower frequencies the spectra are higher in unstable atmosphere and lower in a stable atmosphere. Højstrup has derived a model which can be used in the

unstable and neutral atmosphere. Only one reference was found which gives an experimentally determined coherence function of offshore wind. The parameter values found in the experiment agree well with the values found in literature.

7.3 Wind Data for Wind Energy Production Estimates

7.3.1 Introduction

To estimate the energy yield for offshore wind turbines it is necessary to have a description of the wind climate at hub height for the location where a particular wind turbine will be installed. Because the installation of towers for measuring the wind speed at every possible offshore location is very expensive and time consuming, there is a need to develop procedures to describe the wind climate using existing offshore data. For the calculation of the wind climate it is necessary

1. to compose a map which describes the geostrophic offshore wind climate
2. to translate the geostrophic wind climate at the desired location to the wind climate at hub height

Although the procedure is straightforward, it is not easy to develop such a procedure.

Various methods exist which can be used to compose a map which describes the geostrophic wind climate. These methods differ in complexity and therefore it is necessary to assess the climatological data that are needed first. More detailed information gives a higher accuracy of the estimated energy yields. We can distinguish the following relevant wind climate information (in order of importance):

1. Overall mean wind speed
2. Overall wind speed frequency distribution and Weibull parameters.
3. Mean wind speed and frequency of occurrence per wind direction sector
4. Interannual variations of the wind speed
5. Mean annual course of the wind speed
6. Mean diurnal course of the wind speed.
7. Wind speed frequency distribution per month
8. Wind speed frequency distribution per wind direction sector

For a first rough estimate only the overall mean wind speed is necessary. A better estimate can be obtained when also the frequency distribution, characterized by its Weibull parameters, is taken into account. Other wind climatological data can be used to study specific aspects, for example:

- the wind speed distribution by wind direction, necessary to calculate wind farm losses,
- the interannual variation in wind speed to give some insight in yearly variations in the cash flow.

7.3.2 Geostrophic wind

Maps for the overall wind speed above the North Sea do exist using pressure field data as an input. Since these maps can only supply average wind speeds, these maps cannot be used to give a more detailed description of the wind climate.
For a more detailed description of the wind climate it is also necessary to have information about the wind speed frequency distribution, the distribution by wind direction etc.
Therefore, it will be necessary to describe these aspects also for the geostrophic wind climate, see for comparison Lundtang Petersen et al. [1981]. These data can only be generated by using the surface wind speed data.

The analysis of the different methods, used to calculate the mean geostrophic wind speed from surface wind data for K13 and LV Texel, shows that there is good agreement among the four methods. Further, the spatial variation of the mean geostrophic wind speed between these two stations is small.

These results are very promising. They show that the geostrophic wind speed can be calculated with existing methods from surface wind speed data. However, further validation with data from other measuring stations is necessary to be sure about these conclusions and to check the geographic variation of the geostrophic wind speed. Especially coastal locations, both offshore and onshore, must be taken into account.

The results also show, however, that the Weibull shape factor for the geostrophic wind speed for K13 is not the same as for LV Texel. It is not clear what brings about this difference. Further research using other databases must be carried out to identify the Weibull shape factor for the geostrophic wind speed and the geographical variation. Also other aspects of the geostrophic wind climate require the investigation of wind speed databases of other stations.

7.3.3 The wind profile

For an adequate description of the wind climate it is necessary that the wind climate at heights between 10 m and 120 m can be described (see 7.3.1). One of the main aspects is of course the mean wind profile. The wind profile can be described by a logarithmic function including a stability correction, according to Monin-Obukhov similarity theory, characterized by the roughness length z_0 and the Obukhov length L. Above sea the roughness length can be described by the Charnock relation and is a function of the wind speed. The Obukhov length is a function of the air- and seawater temperature and the wind speed.
There are indications that for wind energy applications the mean wind profile can be simplified by taking z_0 as a constant and assuming $L = \infty$ (neutral).

By calculating the geostrophic wind speed for K13 and LV Texel and from other research [Van Wijk, 1990; Walmsley, 1988] the conclusion is valid that stability corrections do not affect the overall mean wind profile above sea very much (difference in the means within 0.2 m/s for a scaling of 60 meter). However, it

must be kept in mind that other climatological figures such as the Weibull shape factor will be affected by taking into account stability corrections. By calculating the average roughness length for K13 this seems to be very close to the value of 0.0002 m, which is used in various standard text books.

These conclusions are based on a very limited and inappropriate database. Validation of the diabatic wind profile with the West Sole database, turned out to be impossible because of the erroneous seawater database. Therefore, it is necessary to validate the wind profile functions properly. This can be done be setting up a measuring campaign in which the wind speed will be measured at several heights at one station. One of the existing stations in the Measuring Network North Sea can possibly be used for this purpose.

7.3.4 The wind climatology in the coastal transition region

The wind climatology in the coastal transition region was not part of the research in this project. However, a description of the wind climate in this region is very important, because it will probably be one of the first areas where offshore wind turbines will be erected. Research in this area will also give information on the wind climate in the IJsselmeer.
Further, a description of the wind climate in the transition region is important because it opens the way to describe the wind climate above land and above sea with one single methodology. This decreases the probability of anomalies, such as discontinuities in the wind energy production estimates close to the coast.

The problem is that there are very little databases available in the offshore transition region, neither in the North Sea nor in the IJsselmeer. Studies that have been carried out on the subject of the wind profile and internal boundary layer in this transition layer have used onshore databases.
Therefore, a measuring station in this transition layer offshore is necessary. This station must be used to carry out measuring campaigns that can generate databases for studying the wind profile, the internal boundary layer, roughness lengths in shallow water, etc.

7.3.5 Summary

In short a summary of the research that has to be carried out for an adequate description of the offshore wind climate for energy yield estimations is given here:

- Validation of the overall mean geostrophic wind speed using other databases from the Measuring Network North Sea and some selected databases from Light Vessels.
- Composition of maps for the geostrophic wind climate, using the databases from the Measuring Network North Sea: not only a map for the overall mean geostrophic wind speed, but also maps for the Weibull shape factor, the wind speed distribution per wind direction, the mean wind speed per month, etc.
- Validation of the wind profile relations using databases from measuring campaigns, that can be carried out at one of the stations of the Measuring

Network North Sea.
- Examination of the wind climate in the offshore transition region by setting up a measuring station in this transition region which is able to carry out different measuring campaigns.

7.4 Wind data for Wind Turbine Design

The Handbook Wind Data for Wind Turbine Design must be adapted on a number of topics in order to be suitable for offshore load calculations, such as:

1. wind speed frequency distribution,
2. turbulence intensity,
3. applied roughness length z_0,
4. incorporation of stability classes (may be unnecessary).

Provisional data are available from the analysis of the K13 database. Stability has an effect on the turbulence intensity and on the wind shear. However, the average effect of stability might be limited, and could possibly be neglected in the context of the handbook. In order to estimate the effects, it is necessary to analyze turbulence data for various stability classes, based on reliable temperature measurements.

The expressions for the calculation of the fatigue gust amplitudes, which were derived from the wind speed measurements at Cabauw, are probably not valid under offshore conditions. Offshore measurements are necessary to verify the validity of the expressions or to derive new valid expressions. These measurements could be obtained during a relatively brief measuring campaign (the gust analysis in the present handbook is based on 700 hours of Cabauw data).

Since wind speeds are generally higher offshore and turbulence intensities lower it is not exactly known what the final effect is on the extreme wind speeds. A detailed analysis of maximum wind speeds should be combined with estimates of the turbulence intensity at high wind speed in order to obtain the required empirical factors in the handbook

In view of the scarcity of experimental spectra and coherence functions offshore and the uncertainties in the spectra at low frequencies, measurement of these functions is necessary in order to supply the data required by a stochastic wind simulator, such as SWIFT. These data can be obtained during relatively short measuring campaigns.

Finally, in designing wind turbines for offshore conditions it is very important to have design data on sea waves and the interaction of sea waves and wind, especially under storm conditions. This topic has not been part of this study, but it should be addressed in the future.

8 References

[1] Barthelmie, R.J., J.P. Palutikof, T.D. Davies,
Prediction of offshore wind speed -
A comparison of methods, Proceedings BWEA, Norwich, 1990.

[2] Beljaars, A.C.M.,
The measurement of gustiness at routine wind stations -
a review,
KNMI, De Bilt, WR 87-11, 1987.

[3] Børresen, J.A.,
Wind atlas for the North Sea and the Norwegian Sea,
Norwegian University Press, 1987.

[4] De Vries, E.T., J.C. Berkhuizen, M.A.T. Clemens,
Windenergie offshore - een verkenning (in Dutch),
CEA, 9101, Rotterdam, 1991.

[5] Eidsvik, K.J.,
Large sample estimates of wind fluctuations over the ocean,
Boundary Layer Meteorology, **32**, 103-132, 1985.

[6] Garratt, J.R.,
Review of drag coefficients over oceans and continents,
Mon Weather Rev. Vol. 105, pp. 915-929, 1977.

[7] Højstrup, J.,
Velocity spectra in the unstable boundary layer,
J. Atmos. Sci., **39**, 2239-2248, 1982.

[8] Kaimal, J.C.J.C. Wijngaard, Y. Izumi, O.R. Cote,
Spectral charachteristics of surface layer turbulence,
J. Atmos. Sci., **33**, 2152-2169, 1972.

[9] Korevaar, C.G.,
Climatological data of the Netherlands lightvessels
over the period 1949-1980,
KNMI, De Bilt, WR 87-9, 1987.

[10] Korevaar, C.G.,
Climatological data for the North Sea based
on observations by voluntary observing ships
over the period 1961-1980,
KNMI, De Bilt, WR-nr 89-02, 1989.

[11] Lundtang Petersen, E., I. Troen,
The European Windatlas, 1990.

[12] Lundtang Petersen, E., I. Troen, S. Frandsen, K. Hedegaard,
Windatlas for Denmark,
Risø, Roskilde, 1981.

[13] Maat N., Kraan C., Oost W.A.,
The roughness of windwaves,
Boundary-Layer Meteorology, **54**, 89-103, 1991.

[14] Minhinick J.H., Folland C.K.,
The Met Office Historical Sea Surface
Temperature Dataset, London,
Met Office. Met O13 Branch memorandum No 137.

[15] Moore,
10 to 100 m winds calculated from 900 mb wind data,
Proceedings BWEA Cranfield, 1982.

[16] Nicholls, S., C.J. Readings,
Spectral characteristics of surface layer
turbulence over the sea,
Quart. J. R. Met. Soc., **107**, 591-614, 1981.

[17] Panofsky, H.A., J.A. Dutton,
Atmospheric turbulence, Models and methods for
engineering applications,
John Wiley and Sons, 1984.

[18] Van Wijk, A.J.M., Beljaars, A.C.M.,
Holtslag, A.A.M., Turkenburg, W.C.,
Evaluation of stability corrections in wind speed
profiles over the Northsea,
J. of Wind Eng. and Ind. Aerodynamics, 33, 551-566, 1990.

[19] Verheij, F., L. van der Snoek (ed.),
Handboek energie-opbrengsten van windturbines (in Dutch),
TNO-MT, Apeldoorn, 1990.

[20] Verheij, F.J., F.J. Föllings, A.P.W.M. Curvers,
Wind data for wind turbine design,
Version 3, INTRON-Milieuconsult, TNO, ECN, 1991.

[21] Vermeulen, P.E.J., B. Oemraw, J. Wieringa,
Wind tunnel measurements of the flow distortion
near the anemometer positions on Pennzoil K-13A Platform,
TNO-MT, Apeldoorn, 1985.

[22] Walmsley, J.L.,
On theoretical wind speed and temperature profiles
over the sea with applications to data from Sable Island,
Nova Scotia, Atmosphere-Ocean, **26**(2), 203-233, 1988.

[23] Wieringa, J., P.J. Rijkoort,
Windklimaat van Nederland (in Dutch),
KNMI, Den Haag, 1983.

[24] Wills J.A.B., Cole L.R.,
Wind measurements at West Sole, Final report,
BMT Fluid Mechanics Ltd., ETSU WN 5081, 1990.

[25] Wills J.A.B.,
The Offshore Wind Environment at West Sole,
Proceedings EWEC'89, Glasgow.

[26] Witteveen, H.C.L.J., H. van Rees, J.W. Hillebrand,
Meetnet Noordzee, Overzicht locaties en sensoren (in Dutch),
Rijkswaterstaat and KNMI, Hoek van Holland, 1989.

9 Authentication

Name and address of the principal
NOVEM
Contract: 24401 - 1010
t.a.v. E. Luken
Postbus 8242
3503 RE Utrecht

Names and functions of the cooperators
Ir. J.W. Cleijne - research engineer

Names of establishments to which part of the research was put out to contract
University of Utrecht
Department of Science, Technology and Society
Oudegracht 320
3511 PL Utrecht
The Netherlands

Date upon which, or period in which, the research took place
September 1990 - September 1991

Signature

Ir. J.W. Cleijne
project manager

Approved by

Ir. F.J. Verheij
supervisor wind energy

ANNEX 1

Summary of coastal stations, light vessels and offshore platforms

Name	Period	Remarks
Elbe 1		German light vessel
Norderney	from '68	German coastal station
Eemshaven	from '80	mast in ciastal bay
Borkumriff	until 7/'88	German light vessel
Huibertgat	from '80	mast in coastal bay
Lauwersoog	from'68	coastal station
Terschellingerbank	'49-'75	Dutch light vessel
Terschelling	'68-'80	coastal station
Vlieland	'49-'72	coastal station
Kornwerderzand	from '63	coastal station
Texelhors	'70-'73	coastal station
Texel	'50-'76	Dutch light vessel
K13	from '76	offshore platform
IJmuiden	from '53	coastal station
Noordwijk	from '82	offshore platform
Katwijk	'60-'74	mast at sea
Hoek van Holland	from '62	coastal station
Maasvlakte	'86-2'/88	measuring mast near cost
Goeree	'51-'70	Dutch light vessel
Europlatform	from '79	offshore platform
L.E. Goeree	from '72	offshore platform
Roggenplaat	from '71	mast in coastal bay
Schaar	from '80	mast in coastal bay
Oosterschelde	from '80	mast in coastal bay
Noord-Hinder	'54-'80	Dutch light vessel
Vlissingen	from '59	coastal station
Cadzand	from '72	mast at sea
West-Hinder	1/'85-4'87	Belgian light vessel
Shipwash		English light vessel
Smith's Knoll		English light vessel
Dowsing		English light vessel
West Sole	from '78	English offshore platform

List of tables

List of figures